Development of a Drop Tube Furnace for Visualization of Combustion of Fuel Particles

by

Fengming Huang

A thesis submitted to the Graduate Faculty of
Auburn University
in partial fulfillment of the
requirements for the Degree of
Master of Science

Auburn, Alabama
May 14, 2010

Keywords: drop tube furnace, alternative fuels, combustion, visualization

Approved by

Steve R. Duke, Chair, Associate Professor of Chemical Engineering
Gopal A. Krishnagopalan, Professor of Chemical Engineering
Mario R. Eden, Associate Professor of Chemical Engineering
Anton K. Schindler, Associate Professor of Civil Engineering

Abstract

This thesis describes the development of a laboratory-scale burn simulator designed to maximize visualization capability in a combustion furnace with a high degree of control of temperature and particle presence. A specific research goal is to provide an understanding of combustion phenomena under conditions that simulate energy generation processing in cement production, such that alternative fuels can be evaluated as possible replacements for coal and other fossil fuels.

The solid fuels used for this study were coal, wood chips and switch grass. The fuel particles used in the experiments were approximately 100 microns in size. Microscope and scanning electron microscope (SEM) devices were used to obtain images of the fuel particles to display their sizes and shapes.

The thesis presents a description of a drop tube furnace and experiments that were conducted in it to observe and evaluate combustion characteristics and phenomena related to a high-temperature conversion of solid fuels. The design and operating conditions of the furnace were selected to evaluate the effectiveness of alternative fuels wood and switch grass in comparison to coal for application in cement production. A facility was designed and constructed for visualization of solid particles in a drop tube at laboratory room temperature and high temperatures (900 ^{o}C). Three visualization systems with different functions were applied to obtain images of particles in the furnace. The magnifications of different imaging systems were determined. The magnification for the

images of combustion of particles in the furnace drop tube was 2.31 µm/pixel while the magnification of microscope images was 0.30 µm/pixel. The resolution of the combustion images in the vertical direction was 0.031 mm/cycle and 0.050 mm/cycle in the horizontal direction.

A fuel particle injection system is described and shown to be effective at providing a controlled delivery of solid particles to the furnace drop tube. Particles were introduced via a vibrating syringe and flat-tip needle into a water-cooled injection nozzle to drop particles into the heated retort in the furnace. Dropping conditions were different for coal, wood and switch grass particles, and experiments determined that No. 21 gauge needles were best for coal particles while No. 20 gauge needles were best for wood particles and switch grass particles.

Clear and highly resolved images of coal, wood, and switch grass particles undergoing combustion at 900 ^{o}C in air were obtained. SEM and microscope images were obtained of the fuel particles before and after combustion. Images of the burning particles revealed clarity and intensity contrast sufficient to estimate particle and flame size and shape. Particles were infrequently in the camera field of view at the highest magnifications because they meandered as they fell. Nevertheless, the capability of the furnace and imaging system was demonstrated, validating the potential of the system to provide color images for surface temperature measurement of solid particles undergoing combustion.

Acknowledgements

The author would like to thank Dr. Steve Duke for his help and support in this research. He has been an excellent research advisor and motivator. I would like to express my gratitude towards my committee members, Drs. Mario Eden, Gopal Krishnagopalan, and Anton Schindler for their time and assistance in helping me complete this task. I would like to show my deep appreciation to Brian Schwieker for mounting the furnace system and useful technical suggestions to improve the system. I also would like to thank Dr. Oladiran Fasina for providing fuel samples and use of his equipment for particle preparation.

The author would like to thank the U.S. Department of Energy for financial support.

The author would also like to thank all of the undergraduate and graduate students that assisted with the development of the methods and equipment used in this research: Joshua Thompson for developing the imaging system, Jager Livingston for installing the water cooling system, and Rajeshwar Chinnawar, Jingran Duan, Brock Wilson and Brandon Norris for their assistance with the research.

Finally, the author would like to thank his parents for their support through this research. This success would not have been accomplished without them.

Table of Contents

Abstract ii

Acknowledgements iv

List of Tables vii

List of Figures viii

Chapter 1: Introduction 1

Chapter 2: Background 4

2.1 Coal as a Fossil Fuel 6

2.2 Wood as an Alternative Fuel 7

2.3 Switch Grass as an Alternative Fuel 8

2.4 Multi-stage Combustion Process for Solid Fuels 10

2.5 Laboratory Burning Simulators 11

Chapter 3: Equipment and Experiment Procedures 20

3.1 Coal, Wood and Switch Grass as Fuel Samples 20

3.1.1 Coal 20

3.1.2 Wood 22

3.1.3 Switch Grass 23

3.2 Particle Preparation 24

3.3 Microscope and SEM Imaging of Particles 25

3.3.1 Microscope Imaging 25

3.3.2 SEM Imaging 31

3.4 Furnace and Particle Injection Systems 34

3.4.1 Description of Furnace 34
3.4.2 Cooling Water System 38
3.4.3 Particle Injection System 39
3.5 Imaging System 44
3.6 Movie Building 50
3.7 Calculation of Imaging Resolution and Magnification 51
3.8 Furnace Operation 54
Chapter 4: Results 57
4.1 Furnace Operation Results 58
4.2 Particle Dropping Rate at Lab -Room Temperature Results 60
4.3 Particle Combustion at High-Temperature Results 65
Chapter 5: Conclusions 70
Chapter 6: Recommendation for Future Work 72
Bibliography 73
Appendix A: Needle Gauge Comparison Chart 78
Appendix B: Key Specifications of Furnace 79
Appendix C: Kodak SR-500 Motion Corder Analyzer Specifications 80
Appendix D: Nikon D40X DSRL Camera Specifications 81
Appendix E: COHU 2122 Monochrome Video Camera Specifications 82
Appendix F: File Batch 83
Appendix G: Movie Speed Setting 84
Appendix H: Movie Building Procedure 85
Appendix I: Furnace Bake Out Procedure 86
Appendix J: Resolution and Magnification Results 87
Appendix K: Coal Sample Results from ROBERTA Plant 89

Appendix L: Particle Dropping at Lab-room Temperature.....90

List of Tables

Table 4-1: Controller temperature and temperatures in retort…….....59

Table 4-2: Optimum needle delivery system……...61

Table 4-3: Coal particle dropping test with No. 21 gauge needle…….……...62

Table 4-4: Wood particle dropping test with No. 20 gauge needle...…….....…...63

Table 4-5: Switch grass particle dropping test with No. 20 gauge needle…....….....64

Table J-1: USAF 1951 resolution test chart (from Edmund).....…….……..88

Table K-1: Cement plant results of coal samples….....….....89

List of Figures

Figure 2-1: Schematic of furnace designed by Levendis et al.(1992)……..…..…12

Figure 2-2: Schematic of furnace designed by Levendis et al.(1993)……..……14

Figure 2-3: Schematic of furnace designed by Baxter et al.(1992).…….……16

Figure 2-4: Schematic of furnace designed by Rush et al.(1998)……..…..18

Figure 3-1: Sample of ground coal from the Roberta plant……..……...21

Figure 3-2: Sample of wood chips from the Rock-Tenn Company…….……22

Figure 3-3: Sample of hammer-milled switch grass……....23

Figure 3-4: Microscope image of pulverized coal particles (40X)….……..……...…26

Figure 3-5: Microscope image of wood particles (100X)...…….....27

Figure 3-6: Microscope image of switch grass particles (400X)…….....….27

Figure 3-7: Microscope image of chars of pulverized coal (720X)...……..…...….29

Figure 3-8: Microscope image of chars of wood chips (720X)...…….….....29

Figure 3-9: Microscope image of chars of switch grass (720X).…….……...…30

Figure 3-10: SEM image of coal at magnification of 1000X…..……..…...32

Figure 3-11: SEM image of wood at magnification of 1000X……....32

Figure 3-12: SEM image of switch grass at magnification of 1100X....….……32

Figure 3-13: Furnace and controller system.....…….……...….36

Figure 3-14: Schematic diagram of laboratory furnace…….....…….....36

Figure 3-15: Ace quartz retort (left) and ATS quartz retort (right) …….....37

Figure 3-16: Vibration system……..…….…….....41

Figure 3-17: Quartz nozzle……..……...……..…..…….42

Figure 3-18: Quartz injection nozzle with running water…….....……42

Figure 3-19: Stainless steel nozzle……..…….……43

Figure 3-20: Stainless steel injection nozzle with cooling water lines….....……43

Figure 3-21: High-speed camera and view window……..…45

Figure 3-22: Kodak SR-500 Motion Corder Analyzer…….…….…...46

Figure 3-23: Cohu camera with Questar lens…….……..49

Figure 3-24: Ruler.....……...…….……..52

Figure 3-25: Scale on a microscope slide.....…….…….…..53

Figure 3-26: Operating furnace at controller temperature of 900^{o}C.....55

Figure 3-27: Heating zone during operation via view window.…….……..56

Figure 4-1: Schematic diagram of temperature measurement….....……..59

Figure 4-2: Burning coal particles at 856^{o}C ….....…….…..…..67

Figure 4-3: Burning switch grass particle at 856^{o}C.....……..68

Figure 4-4: Burning wood particles at 856^{o}C .....….….....……..69

Figure J-1: USAF 1951 resolution test pattern (from Edmund).....……..87

Figure L-1: Dropping particles at laboratory-room temperature….....……....91

Figure L-2: Dropping coal particles with needle by the angle of 35^{o}.....….…….....92

Figure L-3: Dropping wood particles with vertical needle .....……..93

Chapter 1

Introduction

This thesis describes the development of an apparatus and a technique for the visualization of combustion of particles of solid fuels, including coal, wood and switch grass, in a laboratory scale furnace. The hypothesis is that by observing and evaluating high-resolution and high-magnification images of particles undergoing combustion, burn properties and phenomena can be obtained. The thesis introduces a visualization system used to provide digital images and videos of the burning process for individual fuel particles, as they undergo combustion in a furnace quartz retort through a quartz viewing window. The technique provides a means to compare alternative fuels with coal under controlled combustion conditions. A specific research goal is to provide an understanding of combustion phenomena under conditions that simulate energy generation processing in cement production, such that alternative fuels can be evaluated as possible replacements for coal and other fossil fuels for this industry.

The cement industry is a significant component of the economy of the United States with 39 companies operating 118 cement plants and annual shipments valued at approximately $8.6 billion in 2002 [Portland Cement Association, 2009]. Global cement production is much larger, with U.S. production ranked behind China and

India. The production of cement is energy intensive. It is estimated that energy required to produce one metric ton of clinker can be as much as 4.02 million KJ for pre-heater and pre-calciner dry-process kilns and 6.17 million BTU for wet process kilns [Oss, 2002]. In 2001, 88 million metric tons of cement was produced in the U.S., an increase of 20.45% over the period from 1993 to 2001, while the total U.S. energy consumption for cement production increased 20.52% in 2001 [Jacott et al., 2003]. Because of the high energy consumption of the cement industry, there is a strong motivation to substitute alternative fuels for expensive and non-renewable fossil fuels.

In 2005 researchers at Auburn University and Lafarge North America began a joint study of the impact of using alternative fuels in the cement manufacture process with financial support from U.S. Department of Energy. The research in this thesis contributes to this study.

The important contribution of this research study is the integration of a laboratory-scale furnace and a visualization system. An aspect is placing a camera near the heated zone of interest to allow appropriate focusing for high-resolution imaging of small combusting particles. Another research contribution is the development of methods to control the rate of single-particle falling through an injection nozzle at the top of the furnace.

Visualizations were performed at laboratory room temperature to obtain qualitative information about physical properties of fuel particles. Experiments were performed at high controlled temperature (900 °C) to obtain qualitative information about burning characteristics of solid fuels. Target size of selected solid fuel particles

was 100 microns; this size was chosen to match typical coal particle sizes used for cement manufacturing.

Chapter Two provides a brief background of worldwide energy consumption and the environmental impacts of fossil fuels and biomass alternative fuels, with emphasis on cement production. The physical properties and other characteristics of coal, wood, and switch grass as industrial fuels are discussed. Drop tube and furnace-based visualization studies from other research groups are presented.

Chapter Three provides a description of experimental apparatuses and procedures, and the specifications of the fuel samples used in the research. The imaging acquisition and analysis systems used, the particle feeding systems, and the specialized furnace system are described in detail. Microscope images of raw fuel samples and fuel chars after the combustion, as well as SEM images of raw fuel samples are presented and described.

Chapter Four provides results obtained from furnace and particle injection operation in the form of images and calculation results. Key results include particle injection rates, camera resolution and magnification, and images of combustion of solid fuels.

Chapter Five offers the several conclusions made from the discussion of the experimental results.

Chapter Six gives suggestions for future work in the area of visualization of combustion of solid fuels.

Chapter 2

Background

In cement production, the mixture of raw materials is fed to the pre-heater, in which it is calcinated before entering the kiln. In the kiln, the raw materials are fixed together with the ash of all the feeds used. At the end of the kiln, the flux is rapidly added to form clinker. The clinker is cooled and ground with an appropriate proportion of sulfate to form cement [Taylor, 1997]. In order to increase energy-efficiency and economical aspects, the exact manufacturing process varies from one plant to another [Jackson, 1998]. Some plants run a wet process, in which the raw materials are suspended in water in the process; these plants are very energy-efficient and tend to only be used in plants. Most plants run the dry process where grinding and blending are completed on the dry raw materials before they enter the pre-heater [Kosmatka, 2002].

In cement manufacturing, it is essential in the clinker burning process to keep the kiln temperature between 1400 to 1500 ^{o}C, and the kiln gas temperature is at about 2000 ^{o}C. The solid fuel fed via the burner produces the main flame with the flame temperature at approximately 2000 ^{o}C. Hot kiln gases are piped in to combust the fuel [Keefe, 2003]. Hot gases from the combustion process are then used in the

pre-heater, and the ash, residue and unburned samples are swept into the kiln.

In a modern indirectly fired burner, the combustion flame is shaped and adjusted by the primary air, which is about 10-15% of total combustion air [Karstensen, 2004]. The pulverized fuel is blown into the kiln with the mill sweeping air which acts as a carrier and a primary air.

Alternative fuels include waste wood, used tires, and switch grass, etc. Waste wood and used tires have been applied to replace coal or oil as sources of thermal energy in cement manufacturing process [PCA, 2009].

Fossil fuel usage is a huge contributor to the production of green house gas (GHG) emissions. Hanson [Hanson, 2004] estimated that in 2002, 98% or 5,682 million metric tons of total U.S. carbon dioxide emissions resulted from fossil fuel combustion with approximately 50% from coal fired electrical production and petroleum products usage. Overall, total U.S. GHG emissions had risen by 13% from 1990 to 2002 [Hockstad, 2004]. About 3.4% of global CO_2 emission is from fossil fuel combustion and cement production. U.S. is the world's third largest cement producer, with production occurring in 37 states [EPA, 2004]. In the U.S. combustion-related emissions from cement production were estimated at approximately 36 million ton CO_2, which was about 3.7% of combustion-related emissions in the U.S. industrial sector [United State Geological Survey, 2002]. Expectations are that emissions will continue to rise in the near term.

2.1 Coal as a Fossil Fuel

Coal is a combustible black or brownish-black sedimentary rock, which consists of carbon along with variable quantities of other elements. Coal is the largest source of fuel and is primarily used as a fuel for the generation of electricity worldwide. Coal's combustion is the largest source of CO_2 emission worldwide. CO_2 is the major contributor to increase global warming and other climate changes. The energy density of coal is about 24 MJ/kg [Deutch, 2007].

In general, the traditional process of burning coal in boilers or reactors to drive steam turbines is relatively inefficient with a maximum overall efficiency of approximately 38% [Schilling, 2005]. Coal can be crushed into fine particles, then blown into the boiler, and ignited to form a long flame. It also tends to produce many emissions of nitrogen oxides (NO_X) and sulfur dioxide (SO_2), which is a major source of the formation of destroying ozone and acid rain. In some types of boilers, the burning coal would rest on grates. The typical useful energy output of coal is about 30% [Fisher, 2003].

However, there are several special boilers around the world with high-efficiency. A new technique, called a fluidized bed boiler, made a major improvement in the basic system. Coal in a fluidized bed boiler produced a high pressure stream of combustion gases that spin a gas turbine to generate electricity, and then boil water for a steam turbine - two sources of electricity from the same fuel [Beach, 2009].

2.2 Wood as an Alternative Fuel

Wood is one of the important renewable energy sources produced as manufacturing waste products. The material is generally called fuel wood. Hardwood has less resin and burns slower. Softwood burns quickly [Hoadley, 2000]. It can be made from brush, saplings, waste wood, tree slash as well as from roadside maintenance operations [Redmond, 2006]. Wood has been used as fuel in manufacturing plants and power plants [Maker, 2004], but there are few reports and literature about usage of wood as a thermal energy in cement manufacturing.

The heat content of wood is variable, and mainly depends on its moisture contents. The average energy value of the bone-dry wood chips is approximately 19.8 kJ/kg. However, the actual energy value of any wood sample depends on the mixture of species in the sample and can be measured by laboratory methods [Maker, 2004]. Teislev [2002] reported that wood fuel contains 42% of moisture, typically, and has the following chemical composition: Carbon 50.1%, Oxygen 42.7%, Hydrogen 6.2%, Ash 1.0% and Nitrogen 0.2%. Wood does not have the element of sulfur, so does not produce sulfur oxide gases in combustion, which is different to fossil fuels, but wood combustion will also produce carbon monoxide, nitrogen oxide and volatile organic compound emissions.

Seventy percent of Alabama are covered by forests, and Alabama's forests produce 2.5 times more timber volume now than 50 years ago. From 2001 to 2008, hard wood in Alabama grew by 18.7 million tons annually and soft wood grew by 37.9 million tons annually, for a combined 5.3% increase annually [AFC, 2009].

2.3 Switch Grass as an Alternative Fuel

Switch grass is a warm season grass native to North America, and it is used as a biomass crop and recently as an alternative fuel. It can be found in remnant prairies, pastures and as an ornamental plant in gardens [Sami, 2001].

In some warm humid southern zones such as Alabama, it has the ability to produce up to 25 Oven Dried Ton (ODT)/ha. A summary of switch grass yields across 13 research trial sites in the United States found the top two cultivars in each trial to yield 9.4 to 22.9 ton/ha, with an average yield of 14.6 ODT/ha. Switch grass contains approximately 18.8 billion J/ODT of biomass [McLaughlin, 2005; Samson, 2008].

Now, switch grass is being used as a substitute for coal in power generation and other industrial applications. For example, in Eastern Canada, some plants use switch grass on a pilot scale as a boiler fuel for commercial heating application, and develop switch grass as a pellet fuel because of lack of wood residues [Samson, 2009]. Switch grass has been identified by the U.S. Department of Energy as a possible energy source primarily to be used in existing energy utilities as a feedstock to be co-fired with coal. Dry switch grass's heating value is about 3900 kJ/kg, a fact which results in switch grass having a low energy density when compared to conventional energy sources, but average when compared to other energy crops such as willow [Miura, 2001]. Switch grass can also be directly combusted or co-fired with coal to lower emissions associated with the burning of that fuel. However, for switch grass to become practical as a direct-combusted fuel in coal plants, retrofitting current boilers from coal to co-fired applications is required. The main products from switch grass

combustion are gases and an ash residue.

Though switch grass has been burnt successfully with coal in power plants, it has not been used in a cement plant before. In power plants, some problems will appear during the combustion from elements in switch grass (such as sodium, silica, etc.) due to erosion, fouling and slagging, so decreasing efficiency while increasing maintenance cost [Sami, 2001]. However, in a cement kiln, these problems will not exist because ash can be mixed into the clinker. Hence, switch grass burning is a decent option in cement kilns, if it does not change the properties of the clinker. Another variable affecting the economics of burning switch grass is from the extent of preparation process for switch grass before it is fed into the kiln [Boylan, 2000].

Inherent in the combustion of switch grass is the production of a solid phase residue [Boylan, 2000]. The mass varies from 2-4% of the original sample weight and is primarily composed of metal oxides and ash. If combustion proceeds to completion then the only by-products are CO_2 and water; however, if incomplete combustion occurs, then by-products such as CO, hydrocarbons, NO_X or some other less desirable products are possible. Ash is primarily comprised of silicates and metal oxides and will not undergo combustion at these temperatures but will undergo volatilizations at much higher temperatures associated with the melting points of these components [Yang, 2008].

2.4 Multi-staged Combustion Process for Solid Fuels

Combustion is a multi-staged process, and there is a variation in the combustion of different solid fuels. In general, there are five reaction zones existing in the combustion of solid fuels: 1) the non-reacting solid zone, and solid fuel heats up to approximately 100^{o}C evaporating the moisture in it; 2) the condensed phase reaction zone; 3) the gas phase reaction (pyrolysis) zone, and solid fuel starts to break down converting the fuel into gas at about 300 ^{o}C; 4) the primary (gas phase) combustion zone, and the major energy in the solid fuel is released from 300 ^{o}C to 600 ^{o}C when fuels vaporize containing approximately 40% to 60% of the energy burn; and 5) the post-flame reaction zone. Four basic stages are defined by the concept of solid fuel combustion reaction mechanisms: 1) heating and drying; 2) solid particle pyrolysis; 3) gas phase pyrolysis and oxidation; and 4) char oxidation. Heating and drying occur in the non-reacting solid zone [Tillman, 1981].

Combustion is also a complex process of exothermic chemical reactions between a fuel and an oxidant accompanied by the production of heat or both heat and light in the form of flames or a glow, with an appearance of light flickering. Direct combustion in atmospheric oxygen is a reaction mediated by radical intermediates [Tillman, 1981]. The conditions for radical production are naturally produced by thermal runaway, where the heat generated by combustion is necessary to maintain the high temperature for radical production. Incomplete combustion occurs when there is not enough oxygen to allow solid fuel to react completely during burning to produce CO_2, or when the burning is quenched by a heat sink.

2.5 Laboratory Burning Simulators

Many researchers focus on combustion of solid fuels (such as coal, wood, etc.) and develop laboratory-scale combustion facilities designed to study burn mechanics and chemical analysis. Optical apparatuses are used in this study to visualize the combustion process in the laboratory-scale burn simulator. The drop tube furnaces designed to burn solid fuels and their accessory visualization apparatuses are introduced herein.

Levendis et al. [Levendis, 1992] designed a laboratory-scale furnace to burn particles with a three-color ratio pyrometer to obtain surface temperatures of particles and high-temperature combustion rates of burning carbonaceous particles. They then compared the features and performances of this instrument with those of a two-color ratio pyrometer. They monitored the combustion of particle flow coaxially, from observation windows located at top of the furnace injectors, but not the side view windows as our furnace. Coaxial monitoring is hard to obtain dropping condition and the velocity of the particle, but has the advantage that the whole combustion process can be monitored. A schematic of this furnace is shown in Figure 2-1.

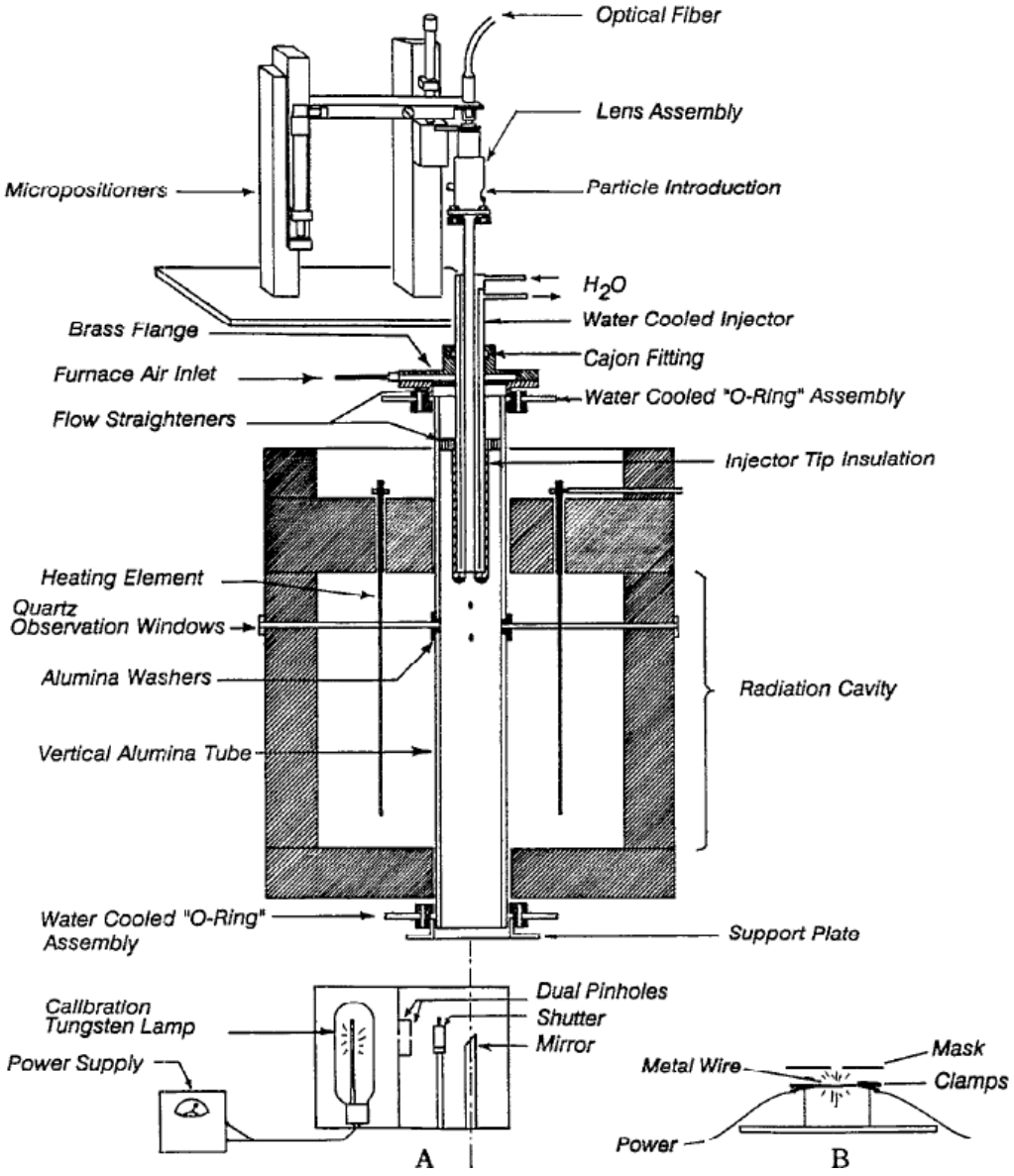

Figure 2-1: Schematic of furnace designed by Levendis et al. (1992).

The temperature-time history of burning particles was recorded by a pyrometer in Levendis' experiment. Narrow (or medium) bandwidth interference filters guide monochromatic radiation to solid-state silicon photo-detectors. The associated amplification is linear and/or logarithmic.

Levendis et al. [Levendis, 1993] designed another type of furnace system to study the combustion emissions from pulverized solid fuels: NO, SO_X and CO. A schematic of this furnace can be seen in Figure 2-2. The particles were burnt in an electrically heated drop tube furnace at high particle heating rates (104-105 K/s) and elevated gas temperatures (1300-1600 K). A small amount of particles were introduced into a test tube from a syringe pump [Wheatley, 1993; Levendis, 1993; Courtemanche, 1998].

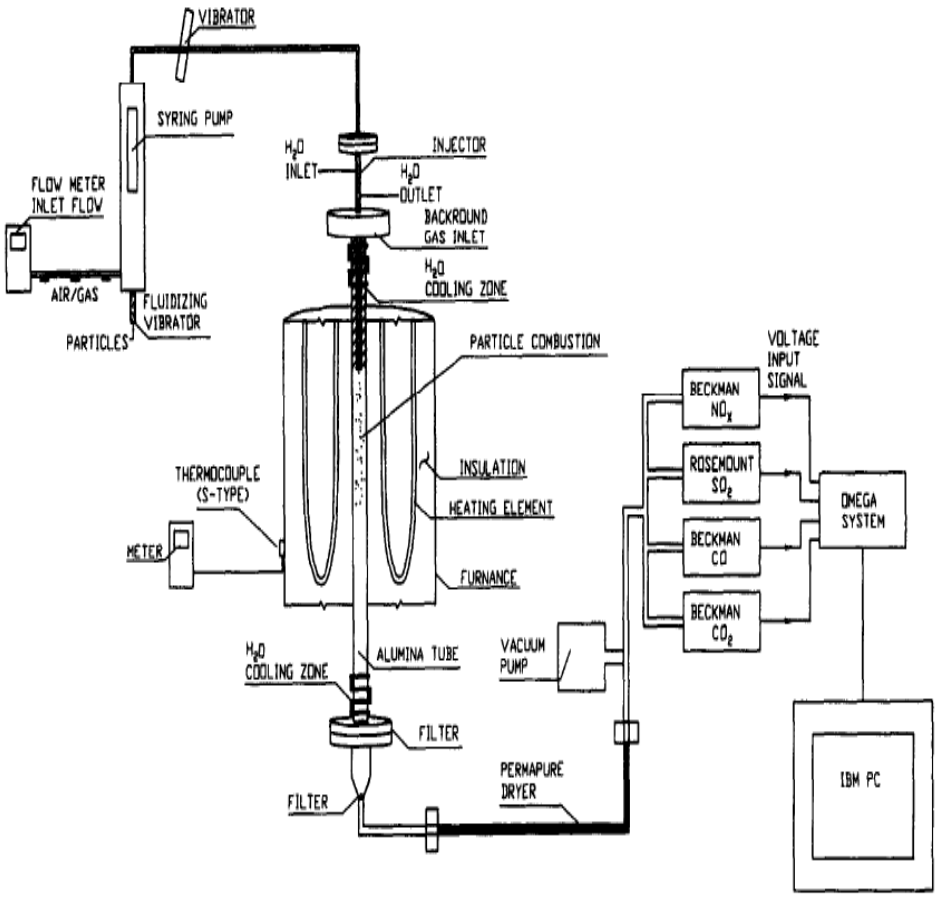

Figure 2-2: Schematic of furnace designed by Levendis et al. (1993).

The particles were dropped via a water-cooled injector. A Type S thermocouple was used to measure the wall temperature and a suction thermometer was used to measure the gas temperature (aspirated shielded thermocouple) in the furnace. The flow rate of the gas was adjusted to provide a calculated gas residence time under different temperatures in the heating zone of the furnace. The furnace gas in their experiment was below 100 ^{o}C at the exit of the furnace.

Baxter et al. [Baxter, 1992] designed a type of furnace to co-fire coal and biomass to valuate the use of the alternative fuels in industrial application. It was a pilot scale, down-fired, turbulent flow simulator as shown in Figure 2-3. Composition histories and gas temperature were tested in the combustion system. The simulator was an electric heating system to control the wall temperature with an inner diameter of 15 cm [Baxter, 1992; Robinson, 2002]**.** Solid fuel introduction rate was 3.5 kg/h through a water-cooled lance inserted at the side of the furnace, which equaled a heat input of 30 kW of bituminous coal. A natural gas-preheated burner was applied to create an air stream.

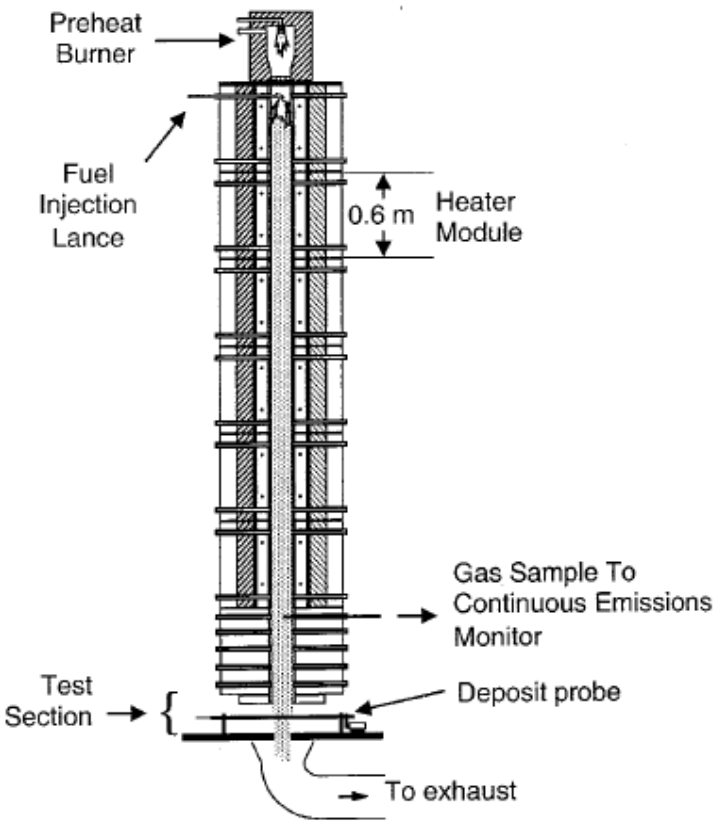

Figure 2-3: Schematic of furnace designed by Baxter et al. (1992).

Ruth et al. [Clean Coal Technology Demonstration Program, 1996; Ruth, 1998] developed a burn simulator in their experiment to study the combustion of coal and municipal solid waste (MSW) in terms of fuel characteristics, combustion technologies, emissions, and ash utilization/disposal showed in Figure 2-4.

However, most of the previous studies focused on measurement of the relationship between combustion temperature and time as well as the measurement of chars and emissions after the combustion, while few studies focused on the visualization of combustion characteristics. In this thesis, particle injection, temperature distribution and particle combustion phenomena were evaluated.

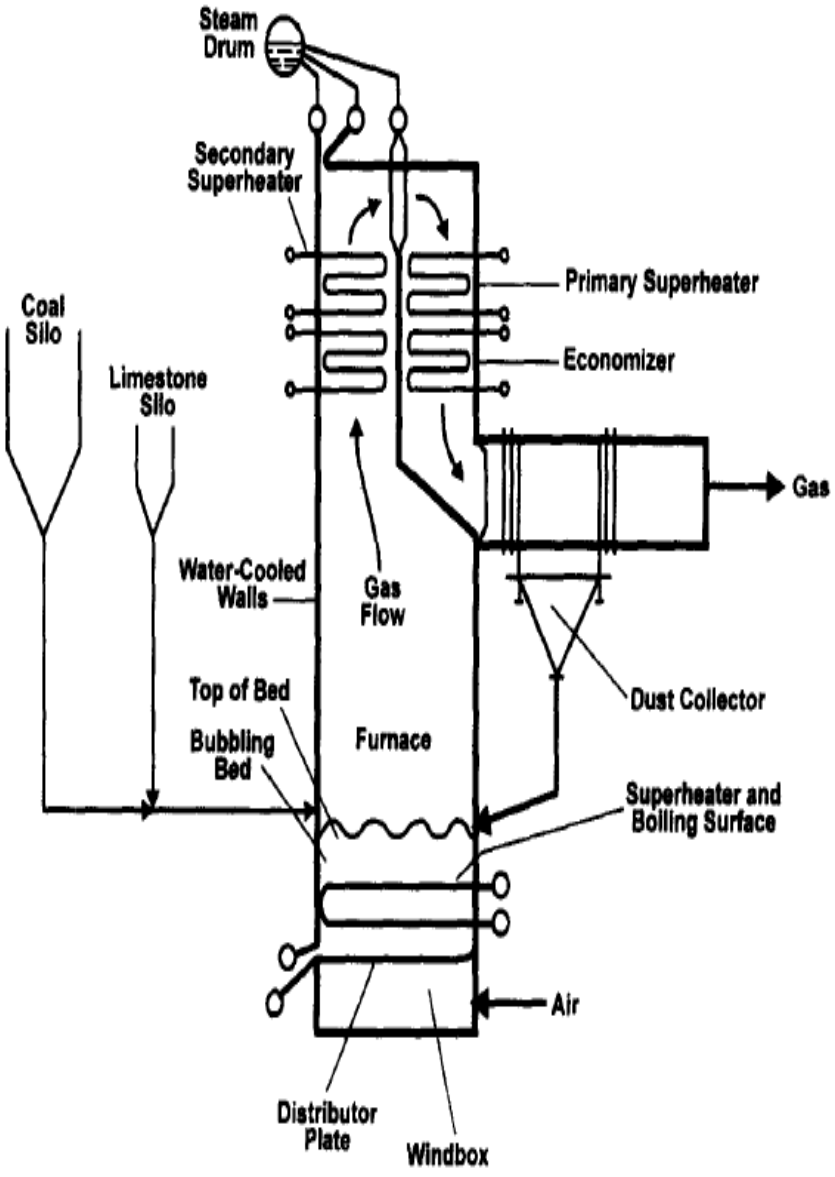

Figure 2-4: Schematic of furnace designed by Ruth et al (1998).

For the coal particle injection and combustion, immediately after its introduction into the furnace, the fuel was rapidly heated by radiation from the combustion process and by convection from the hot furnace gases. Any moisture in the fuel was driven off, followed by a process in which volatile material evolved from the fuel, ignites, and burns. Finally, the fixed carbon in the devolatilized fuel particles was ignited. The composition of coal provided to the burners of a combustion system might vary from hour to hour, or even minute to minute, in the content of volatiles, total carbon, sulfur, moisture, etc [Clean Coal Technology Demonstration Program, 1996].

Fuel particle feeding is a major step in combustion process, and the method to introduce the particle into the burner controls the particle dropping rate. While gas flow is used as a force to drop the particle into the burner, vibrating system can be discussed in later chapters in this thesis.

The visualization (capturing still images and videos) of particle combustion is a method to estimate the characteristics of particle combustion, such as the outer shape of burning particles, temperature distribution during combustion and the characteristics of chars and unburned samples. Meanwhile, the magnification, the resolution, and other specifications of the camera system will affect the quality of the visualization process. It is necessary to adjust these settings to a proper value to obtain better experimental data during the operation.

Chapter 3

Equipment and Experiment Procedures

3.1 Coal, Wood and Switch Grass as Fuel Samples

Pulverized coal, wood chips and switch grass are the materials of interest for the combustion studies performed in this study. Wood chips and switch grass are the alternative fuels, while coal is the standard fossil fuel burned as a comparison.

3.1.1 Coal

The pulverized coal samples were supplied by the Lafarge North America, Inc. Roberta cement plant in Alabama. A picture of the ground coal used in this study is shown in Figure 3-1. Analytical results from cement plant materials testing showed that, on a dry-coal basis, the values (wt.%) of ash, fixed carbon and volatile matter were 18.78, 53.85, and 27.37, respectively. The heat value is 6,761 kcal/kg. The detailed analytical reports are shown in Appendix K.

Figure 3-1: Sample of ground coal from the Roberta plant

3.1.2 Wood

The wood chip samples were southern sweet gum trees, supplied by Rock-Tenn Company in Georgia. A picture of the wood chips used in this study is shown in Figure 3-2. The samples were field dried to be ground into pulverized particles by a grinder machine (Model: OII 350S) from GRAEGER company.

Figure 3-2: Sample of wood chips from the Rock-Tenn Company

3.1.3 Switch grass

The switch grass samples were from the E.V. Smith Research Center of Auburn University, and consisted of the whole plant material, or the entire leaf and stem. The plants were from a lowland variety called "Alamo". The shape of switch grass was very inregular and tangled. The samples were ground with a hammer mill making the size of most particles between 0.5-1 mm. A picture of the switch grass used in this study is shown in Figure 3-3.

Figure 3-3: Sample of hammer-milled switch grass

3.2 Particle Preparation

The ground coal, as received from the Reberta plant, was screened for about 15 minutes using sieves with a shaker (Retsch AS 200). The sieves were Fischer sieve trays No. 40, No. 60, No. 100, No. 140, No. 170, and No. 200. The size fractions were approximately: larger than 400 µm, from 400 µm to 250 µm, from 250 µm to 150 µm, from 150 µm to 106 µm, from 106 µm to 90 µm, from 90 µm to 75 µm, and smaller than 75 µm. The samples were stored in a desiccator to ensure they remained dry.

The wood chips were screened by the same series of sieves used for the coal. The pulverized particles were dried in an oven at 100 ^{o}C for 10 hours and were then stored in sealed Ziplock bags to ensure they remained dry. The hammer-milled switch grass particles were further ground by a coffee grinder to obtain smaller particles. These particles were then screened by sieves to select different sizes of particles (used the same method that applies to coal). The selected switch grass particles were dried in an oven at 100 ^{o}C for 10 hours and stored in Ziplock bags for dryness.

The size of most ground coal burned in the cement plant (full scale test burns) was between 70-100 µm, and coal particles were used as a basis in the experiment. Hence, the visualization system was designed for a particle at 100µm. The size fraction of the particles (including coal, wood and switch grass particles) used in the experiments was between 90-106 µm for better comparison of combustion performance, although waste wood and switch grass were used in larger forms in the cement plant. The other size fractions of particle were stored for possible future use.

3.3 Microscope and SEM Imaging of Particles

Microscope and SEM analyses were performed to observe the outer structure of the different fuel particles.

3.3.1 Microscope Imaging

Pulverized coal, wood chips and switch grass samples were placed on microscope slides. The sizes of the particles selected were between 90-106 µm, and the particles were analyzed using a microscope manufactured by National Optical. Slides were mounted on the microscope and imaged with a Canon digital camera. The camera was connected to a computer, so that it could be controlled by the software to adjust, focus and capture the photographs.

Each slide had many particles, and was viewed at 40 times (40X) magnification (low magnification), 100 times magnification (100X), 400 times magnification (400X), and 1000 times high magnification (1000X). Five images at 40 times (40X) as well as five at 400 times (400X) were taken of each microscope slide sample. Frames of a ruler were captured on the microscope slides to establish scale. The focus was kept in the same position while imaging the particle samples in order to maintain the same scale.

Figures 3-4, 3-5 and 3-6 show microscope images of solid fuel particles. The corresponding scales are shown on the images.

Figure 3-4 is an image of pulverized coal particles at 40X magnification. The image clearly shows that dry coal particles tend to agglomerate, instead of separate.

Figure 3-5 is an image of wood particles with the magnification of 100X. This image shows that the wood particles have consistent structures.

Figure 3-6 is an image of switch grass particles with the magnification of 400X. This image shows that most of the particles are quadrate, instead of rounded.

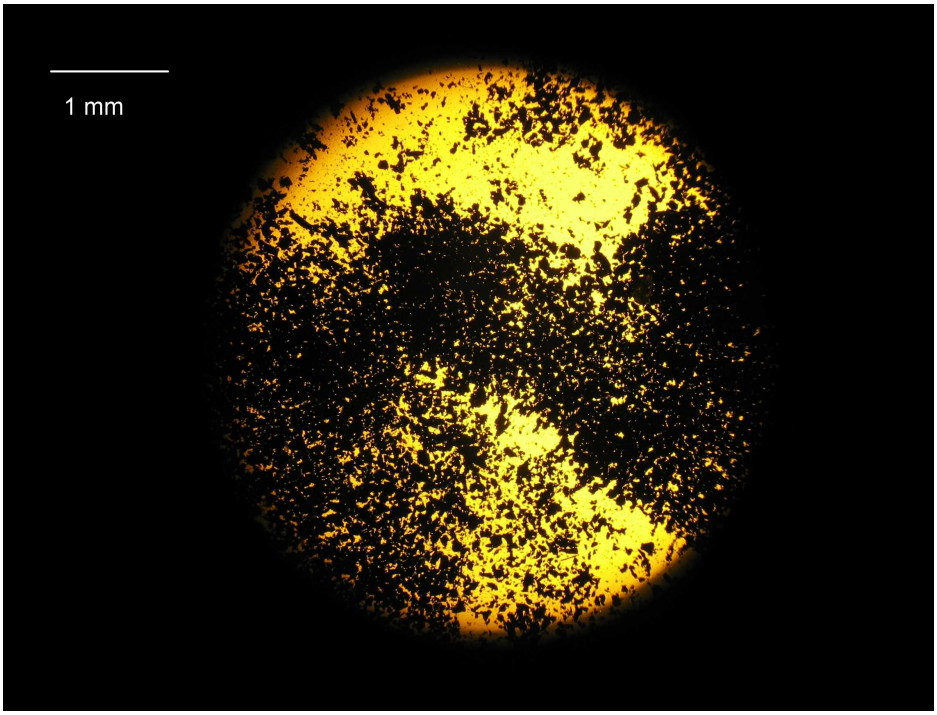

Figure 3-4: Microscope image of pulverized coal particles (40X)

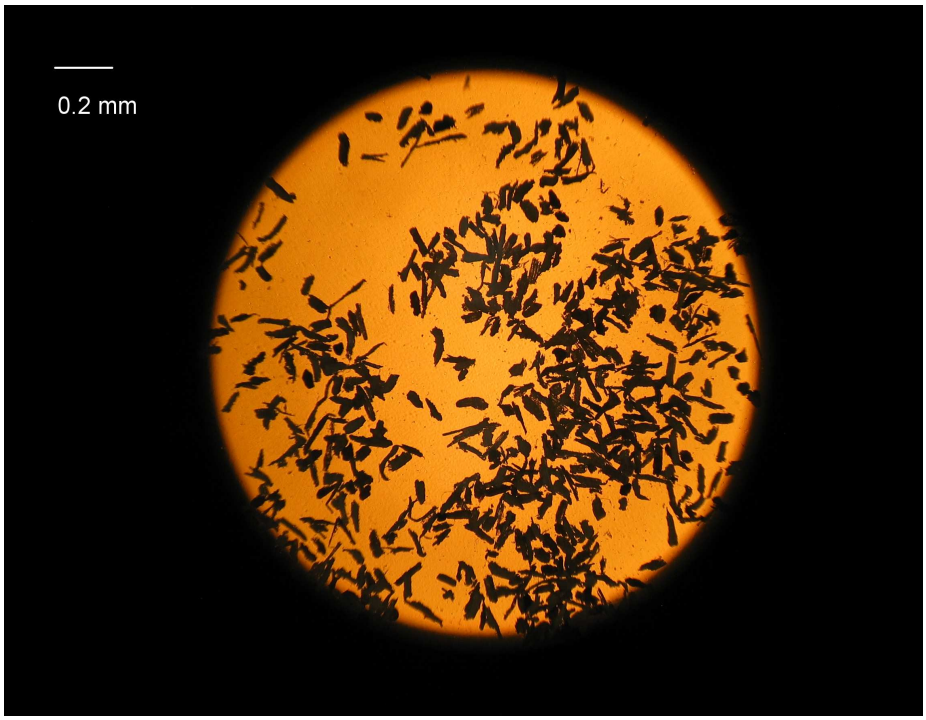

Figure 3-5: Microscope image of wood particles (100X)

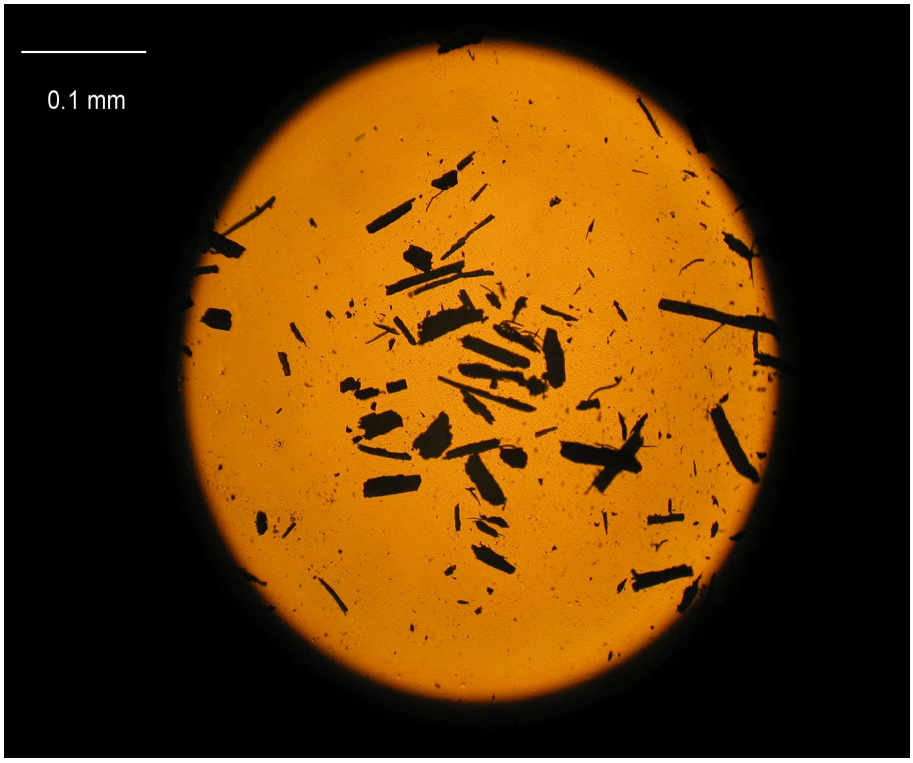

Figure 3-6: Microscope image of switch grass particles (400X)

During combustion experiments, unburned particles and chars dropped onto the cap at the bottom of the retort and deposited there. Char samples of different fuels were selected and placed on microscope slides. Five images at 72 times (72X) as well as five at 720 times (720X) were taken of each microscope slide sample. The focus was kept in the same position while imaging the particle samples to maintain the same scale. Figures 3-7, 3-8 and 3-9 show images of chars of solid fuels under high magnification (720X) on the microscope. The corresponding scales are shown on the images.

Figure 3-7 is an image of chars of pulverized coal. The image shows that coal chars look like big agglomerates. Their color is black, and is same as uncombusted coal particles. Visual observation of many coal chars under the microscope showed that the size of most chars was about 50 µm, when the assumed size of pulverized coal particles was 100 µm.

Figure 3-8 is an image of chars of wood particles. The image shows that different sizes of chars occurred due to different extents of combustion or different initial sizes of particles.

Figure 3-9 is an image of chars of switch grass. The image shows that, after burning, most of the chars look like agglomerates, but are not quadrate in shape.

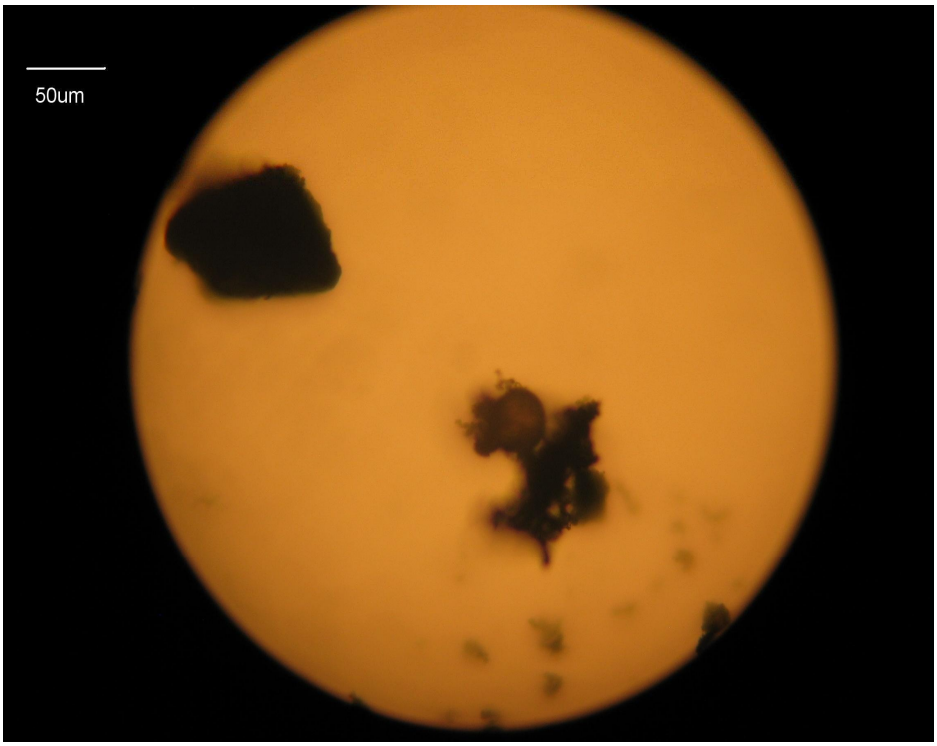

Figure 3-7: Microscope image of chars of pulverized coal (720X)

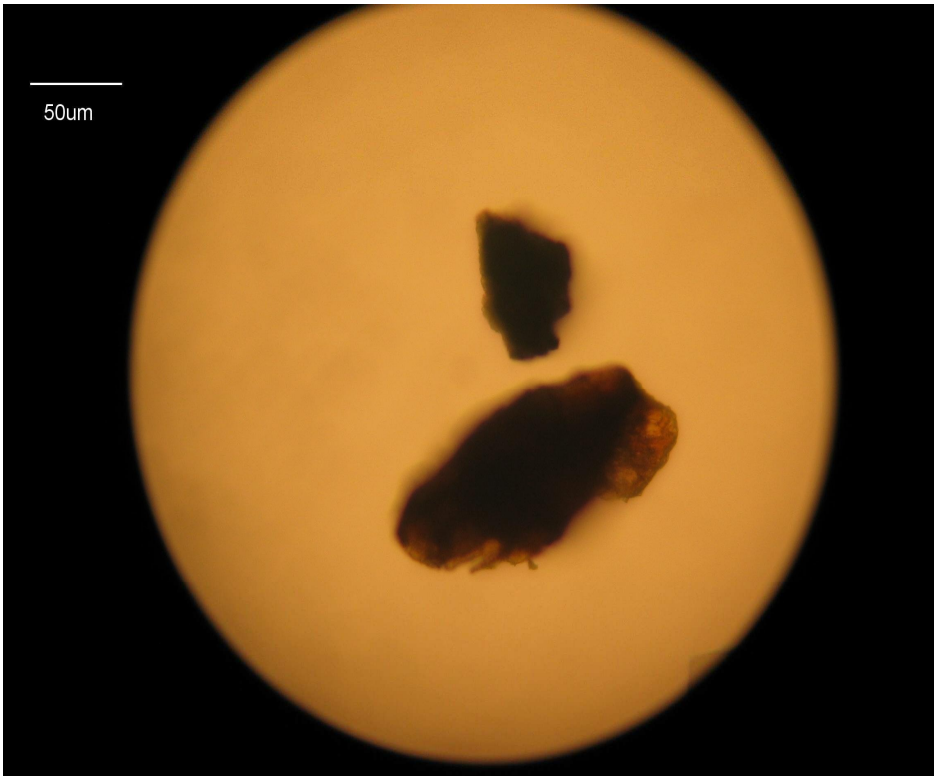

Figure 3-8: Microscope image of chars of wood chips (720X)

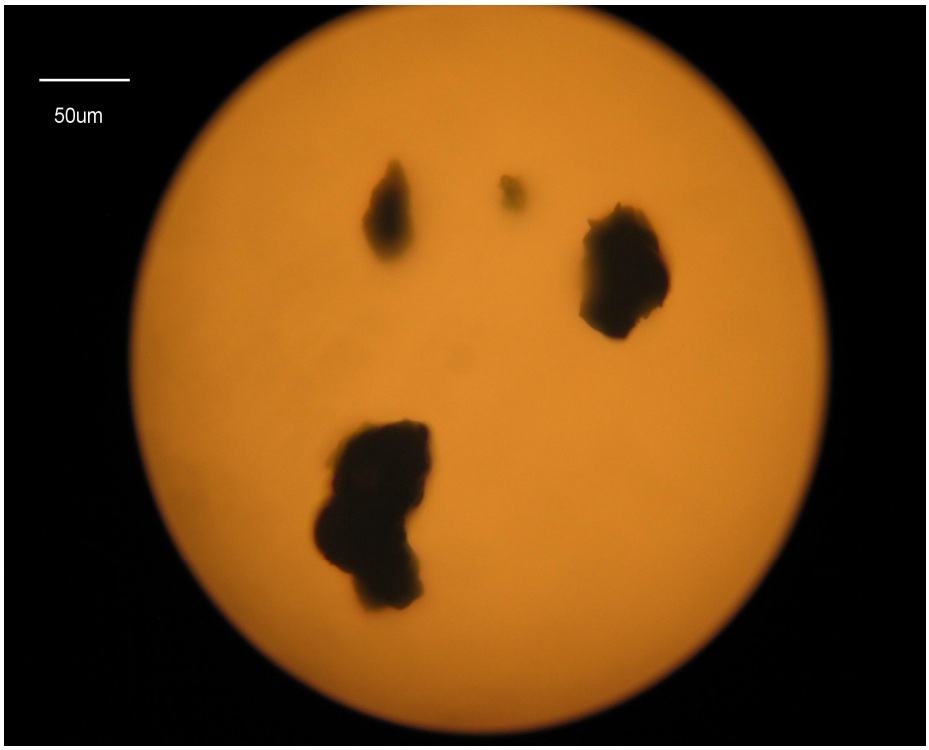

Figure 3-9: Microscope image of chars of switch grass (720X)

3.3.2 SEM Imaging

SEM images were captured using a ZEISS SEM manufactured by Carl Zeiss SMT, Inc. SEM is a useful technique widely applied in visualization of combustion [Atal, 1995]. The SEM machine is located in the Advanced Microscopy and Imaging Laboratory of Auburn University.

The SEM images provided valuable qualitative data to help analyze the prepared solid fuel samples. Figures 3-10, 3-11 and 3-12 are SEM images of pulverized coal, wood chips and switch grass particles, respectively.

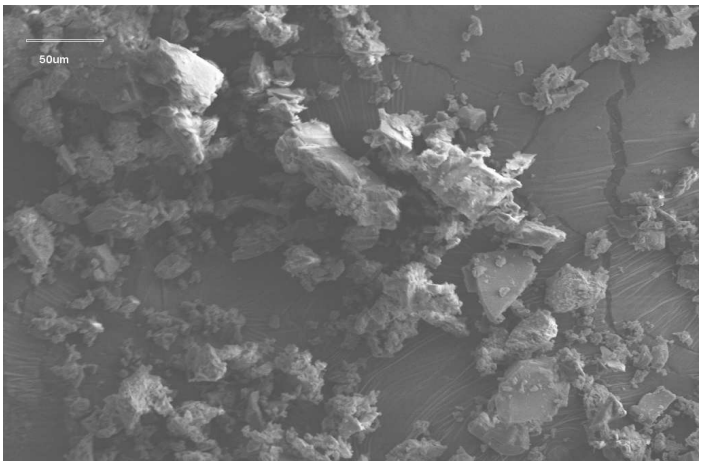

Figure 3-10: SEM image of coal at magnification of 1000X

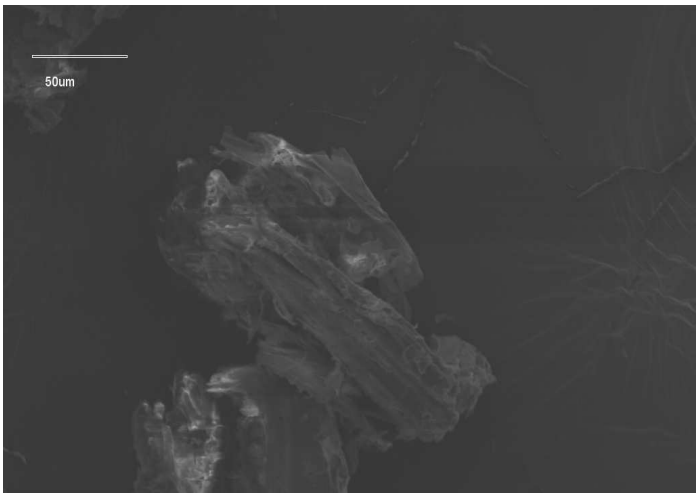

Figure 3-11: SEM image of wood at magnification of 1000X

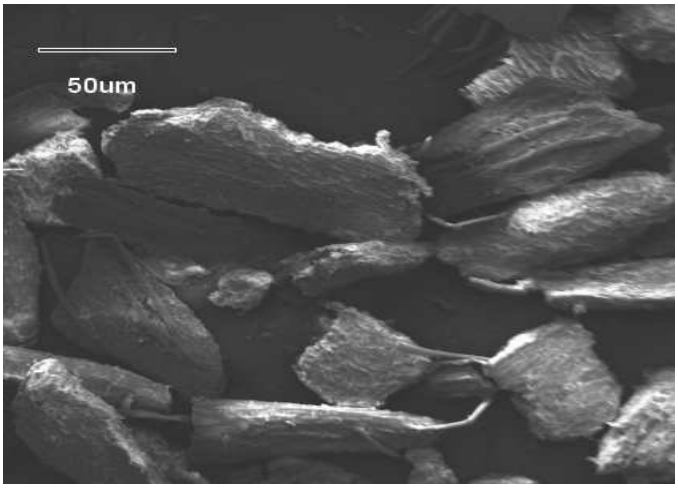

Figure 3-12: SEM image of switch grass at magnification of 1100X

Figure 3-10 is a SEM image of pulverized coal particles at a magnification of 1000X. The image shows that the shapes are variable with a large amount of small dust. Figure 3-11 is a SEM image of wood particles at a magnification of 1000X. The image shows that most of the particles are rectangular with a size of approximately 100 µm. Figure 3-12 is a SEM image of switch grass particles at a magnification of 1100X. The image shows that some particles are irregular in shape.

3.4 Furnace and Particle Injection Systems

The drop tube furnace and particle injection method that was developed for this thesis are two main components in the combustion system. Drop tube furnace systems are relatively inexpensive to operate and can generate multiple data sets in a short time. Of utmost importance is the ability of these systems to simulate key full-scale combustion conditions. Visualization devices include cameras (high speed camera, high resolution camera and regular camera), lenses, computers and imaging processing software.

3.4.1 Description of Furnace

The drop tube furnace was manufactured by Applied Test Systems, Inc. It is an ATS Series 3420 split- tube furnace mounted vertically. The dimensions of furnace are 32.5 cm wide, 35 cm across, and 75 cm high. Figures 3-13 and 3-14 show photographs and a diagram of the furnace system. Appendix B displays the Series 3420 product description provided by ATS. The maximum furnace temperature rating is 1450 ^{o}C. There are three heating zones with a total power capacity of 8000 Watts. There are three quartz view windows located on two sides of the furnace with one window centered on one of the side split lines and two windows located near the top and bottom of the split line on the other side. Each view window is 22.5 cm long and 2.5 cm wide. This window arrangement allows visualization of along the full length of the drop tube. A quartz glass retort is mounted in the center of the furnace, supported by flanges at both ends of the retort tube. The flanges are made of stainless

steel and are water-cooled. The flanges are parts of a retort end-cap assembly that includes inconel radiation shields that extend into the retort. The whole furnace weights 90 kg, and it is mounted with carriage bolts to a bracket. The bracket was mounted to a steel roller cart for some experiments and to a fixed structure aluminum frame for other studies. Levendis [1992] used a similar furnace to burn carbonaceous particles.

The furnace has four heating elements located inside the refractory box and adjacent to the retort. The quartz retort is 6.25 cm in outer diameter and 90 cm long. The quartz retorts provided by ATS were manufactured such that the outer surface of the tube had slight undulations; the refraction due to these undulations resulted in blurred images. A retort was obtained from Ace Glass that had smooth inner and outer surfaces to allow for better imaging. ATS quartz retort and Ace quartz retort are shown in Figure 3-15, the left retort was Ace quartz retort while the right one was ATS quartz retort. The undulations of the ATS retort are clearly evident.

The temperature-control system has three Series 2404 Barber Colman Programmable controllers manufactured by Eurotherm. This system allows temperature control in three different heating zones. The heating rate in each zone can be controlled independently. The blue electronics cabinet shown in Figure 3-13 contains the controls system.

Figure 3-13: Furnace and controller system

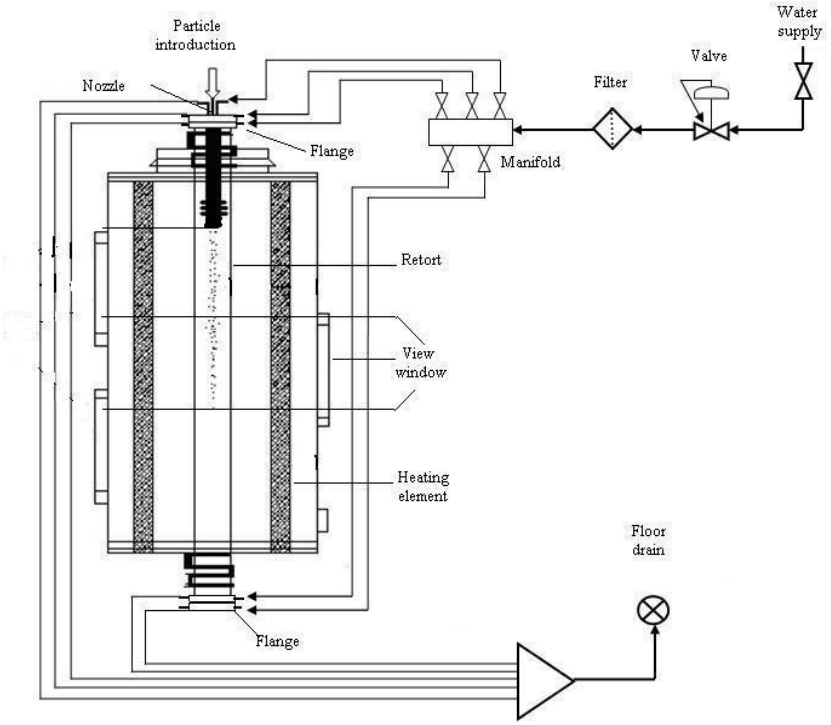

Figure 3-14: Schematic diagram of laboratory furnace

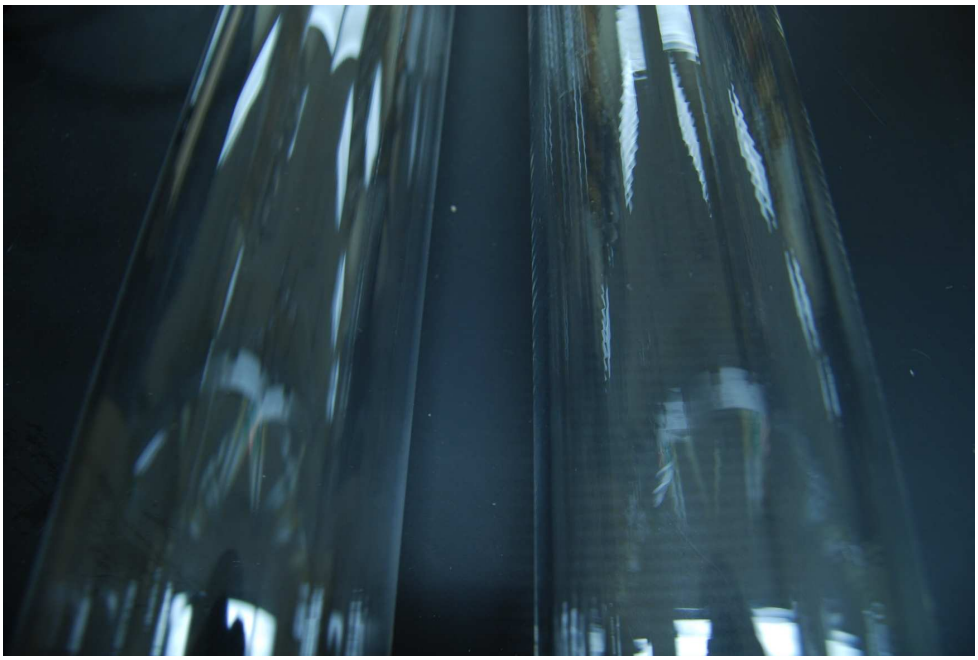

Figure 3-15: Ace quartz retort (left) and ATS quartz retort (right)

3.4.2 Cooling Water System

In order to keep the injection nozzle and flanges cool and to prevent particle burning in the nozzle, a cooling water system was required. The cooling water system was designed by Jager Livingston [Livingston, 2010] to supply water to the flanges of the retort and to the particle injection nozzle. The water cooling system is shown in Figure 3-14. The water supply goes through a filter to remove impurities to keep the fouling in the flanges and nozzle to a minimum. Water enters a manifold that splits it into five lines. One line goes to the injection nozzle, two lines go to the flange at the top of the retort, and two lines go to the flange at the bottom of the retort. Valves allow independent adjustment of the supply to the whole system as well as the flow rate to each individual line.

3.4.3 Particle Injection System

The particle injection system has two main components: a vibrating needle apparatus to control the rate at which particles are dropped, and a water-cooled nozzle to keep particles cool and to prevent them from combusting as they fall through the top of the furnace. The radiation shields and the top of the uppermost visualization window are approximately 20 cm below the top of the furnace. A quartz nozzle and a stainless steel nozzle were designed and tested, and both are described in this section.

The vibration system that was developed to deliver particles from an injection needle is shown in Figure 3-16. The vibrator and controller were manufactured by FMC Technologies (Model: V-2-B). The vibrator was fixed to a metal stand base approximately 2 cm from the stand rod. Approximately 0.2 gram of fuel particles were placed in a 15-mL luer-tip glass syringe. Different gauges of stainless steel flat-tip needles were used depending on the types and sizes of particles. The syringe and needle were from Fisher Scientific. The syringe was clamped to the rod of the vibration stand and the angle of the syringe could be changed at the clamp. As will be discussed later, a specific needle size, angle, and vibration intensity were selected for each fuel type to achieve a suitable delivery rate. The needle tip dropped particles into the top of a furnace injection nozzle.

A quartz nozzle was designed and constructed in the Auburn University Glass Shop. A 6-mm quartz tube was jacketed with a 16-mm quartz tube and the ends of these tubes were sealed together. A second 6-mm tube was located in the cooling

jacket space and provided a connection for water to be able to flow down to the bottom of the cooling jacket. A 7-mm water outlet connection was located at the top of the jacket. The centered small tube served as the particle dropping tube and was open at the top and bottom. The nozzle is shown in Figures 3-17 and 3-18. The quartz nozzle was mounted to the furnace end cap assembly such that it extended slightly beyond the radiation disks, with the top of the nozzle 6.25 cm above the cap and the bottom of the nozzle at 20 cm below the cap. Holes were cut into the radiation disks to allow the nozzle to be inserted. The inner diameter of the dropping tube was 4 mm and the inner diameter of the inlet of water was 5 mm while the outer diameter of whole nozzle was 2 cm. Because of the different heating characteristics of the quartz and stainless steel radiation disks, insulation paper was used to prevent direct contact between the quartz nozzle and the radiation disks. The quartz nozzle proved to be too fragile and broke on several occasions, but it served as a first test of feasibility for the water-cooled injection nozzle concept.

A stainless steel nozzle was designed and constructed in the Chemical Engineering Machine Shop. Based on a similar design rationale used for the quartz nozzle, two small steel tubes were mounted in a large tube and welded together. One was the drop tube for the particles to fall through and the other was the inlet for cooling water. This nozzle was mounted directly to the flange at the top of the retort, with the top at 6.25 cm above the cap and the bottom at 20 cm below the cap. The inner diameter of the dropping tube was 3 mm and the inner diameter of the water inlet was 5 mm. The outer diameter of the whole nozzle was 4.5 cm. No insulation

paper was required with this nozzle, because the radiation disks were welded directly to the jacket of the nozzle, and since all of the material was metal, expansion differences were negligible. The stainless steel nozzle is shown in Figures 3-19 and 3-20.

As discussed previously, the cooling water was supplied and controlled by a valve on the manifold of the water system supplying the jacket and the retort flanges.

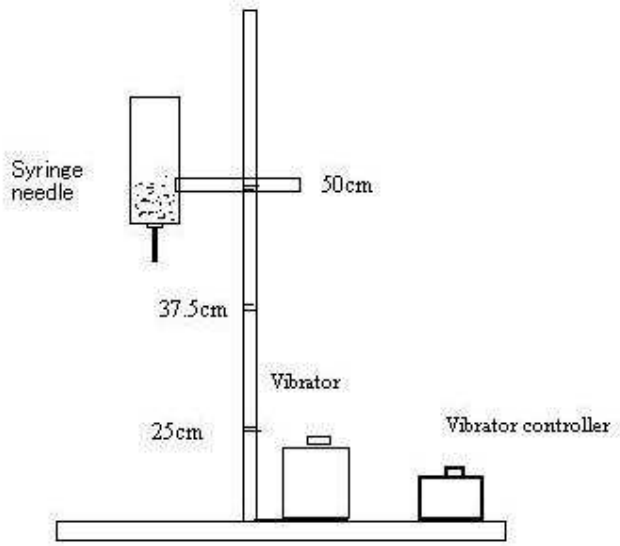

Figure 3-16: Vibration system

Figure 3-17: Quartz nozzle

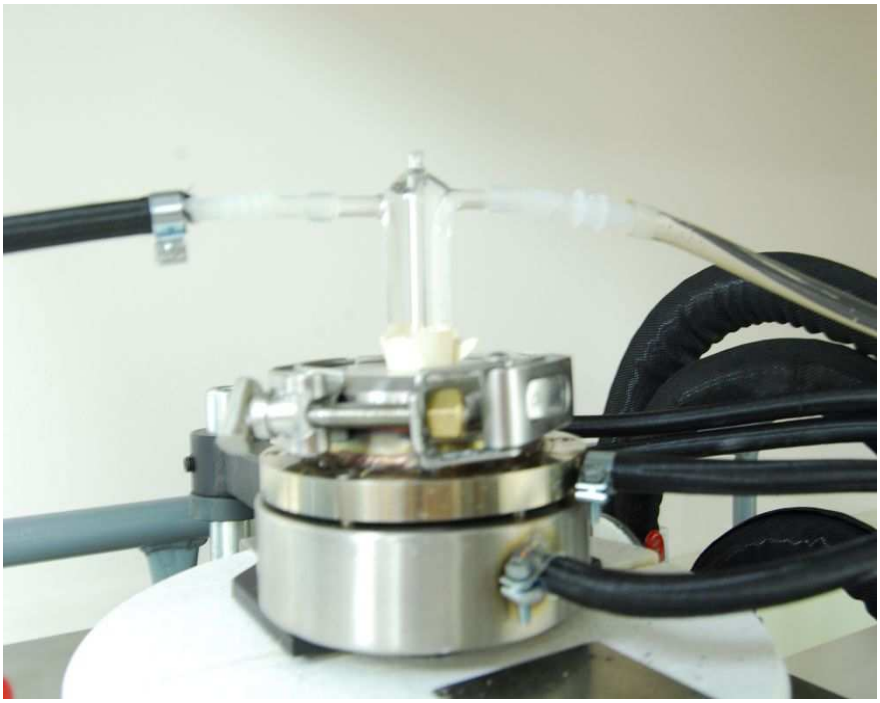

Figure 3-18: Quartz injection nozzle with running water

Figure 3-19: Stainless steel nozzle

Figure 3-20: Stainless steel injection nozzle with cooling water lines

3.5 Imaging system

Three imaging systems were used for the visualization of the combustion of particles studies. One is a standard digital SLR system that employs a NIKON D40X camera (10 Megapixel) with four different lenses, including a Nikon 60 mm F/2.8D AF micro-Nikkor lens, a Nikon 17-55 mm F/3.5-5.6G AF-S lens, a Nikon 50 mm F/1.8D lens, and a Nikon 24 mm F/1.8D lens all with different sets of filters.

In general, the Nikon camera was operated in Manual mode to capture images. The shutter speed was set to 1-10 per second for targets in weak background light and 50-100 per second for targets in strong background light. The size of the image was 3872 x 2592 pixels (10.0 Megapixel).

Some of the images were acquired with a high speed imaging Kodak SR-500 Motion Corder Analyzer with two halogen light sources. The camera worked with a professional SONY video monitor and a computer. The system is shown in Figures 3-21 and 3-22. A 100-Watt incandescent lamp was used with the Kodak camera for back lighting to create a strong white background so that the particles could be better seen and brought into focus. The distance from the lens to the target was 20-37.5 cm.

Figure 3-21: High-speed camera and view window

Figure 3-22: Kodak SR-500 Motion Corder Analyzer

The Kodak camera had a maximum resolution of 512x512 pixels non-interlaced with a rate of 250 frames per second. Focus lenses consisted of several Nikon Nikkor lenses, which could supply detailed shots with a field of view of 9.4 cm^2 and wide shots with a field of view of 25 cm^2. The camera had memory to record 1365 frames, which equaled to about 5.5 seconds of video. Then the onboard frames were transferred to the computer through a SCSI connection. Jasc Animation Shop 3 was used for building the movies from individual frames. The camera system had been used for other studies in Prof. Duke's research group [Davies, 2000; Emerson, 2006; Tuin, 2008].

The Kodak camera was mounted to a tripod and camera rail, which allowed vertical and horizontal camera and lens positioning relative to the retort. The tripod could be raised and lowered to position the camera at each of the different heights of the three view windows of the furnace.

A USAF 1951 resolution test pattern was used to determine image resolution and a scientific ruler was used to determine magnification; these were also used for other visualization systems [Roy, 2001; Emerson, 2006].

The last device is a high resolution monochrome video system: a Cohu 2122 CCD camera and a Questar QM 100 MK III long distance microscope lens. The Cohu camera had 768 x 494 pixels with a pixel size of 8.4 x 9.8 microns. The rate was set for 30 frames per second. The Questar QM 100 had a working distance ranging from 8-35 cm. An available adapter allowed attachment to any F-Mount camera. The camera system was modified from a similar one designed by Amendi Stephens, a

former MS student in Prof. Duke's research group. Stephens [2003] set up the system to visualize the particle formation processes in supercritical fluids.

This system had been applied to view particle dropping and combustion in the furnace. The Cohu camera is shown in Figure 3-23 with the Questar lens attached. The Questar was equipped with both manual and motorized focus. Manual focusing can be done by the focus knob located on the front and rear corners of the lens. The motorized focusing consisted of a hand control, motor and power supply. A top port on the lens allowed open viewing of the field and targets in the microscope.

Figure 3-23: Cohu camera with Questar lens

3.6 Movie Building

The Kodak camera system captures and stores still images. It is necessary to build a movie from still images obtained in the experiments. The detailed procedures are shown in Appendix F, G and H. The built movie is stored as a video clip while the still images are stored as JPEG files.

3.7 Calculation of Imaging Resolution and Magnification

Resolution and magnification are two main characteristics of a camera system. After an image is taken, it is necessary to find the resolution and magnification in the horizontal and the vertical directions.

An Edmund Scientific USAF 1951 resolution test pattern and a scientific ruler were used to determined resolution and magnification. A test chart (Table J-1) was used to calculate the resolution of the camera and analyze the images of the dropping particles. Images of the USAF 1951 resolution target were captured with the target place in the plane where the patterns were in focus. On the USAF resolution test target, the pattern consists of numerous groups of three-bars with dimensions from large to small. The smallest visual three-bar that the image can discern is the limitation of the resolving power in the experiment.

The target format consists of six "groups" in three layers of patterns. The largest groups, forming the first layer, are located on the outer sides of the pattern. The smaller layers repeat the same pattern but are progressively smaller toward the center. Each group consists of six elements, numbered from 1 to 6. Within the same layer, the odd-numbered groups appear contiguously from 1 through 6 from the upper right corner. The first element of the even-numbered groups is at the lower right of the layer, with the remaining 2 through 6, at the left.

As the resolution test usage rule, images were obtained of the target; these were analyzed to determine the three-bar set in a certain direction on the chart that is smallest and resolved, which in this case means showing all three bars separately,

not a solid square shape. Group and Element bar set is chosen on the image, and "cycles/mm" chart (Figure J-2) can be used to calculate the resolution of the camera [Edmund Scientific, 2009]. Hence, the resolution of the image in the vertical was 31µm. In horizontal, the resolution of the image was 50µm.

The ruler was vertically inserted into the retort in the furnace, and part of the rule was located in the field of view of the camera while the camera was set up in front of the view window with the distance of 13 inches to the ruler. The value of line length measured by ImageJ was the value of pixels, but not the actual length. The unit on the rule is 0.416 mm, and the pixels of the image were 640 x 480. The actual length of one unit on the image (shown in Figure 3-24, captured by COHU camera and Questar lens) was 180 in vertical while the actual length of image in vertical was 480, so it could be calculated that the magnification of the image is 2.31µm/pixel.

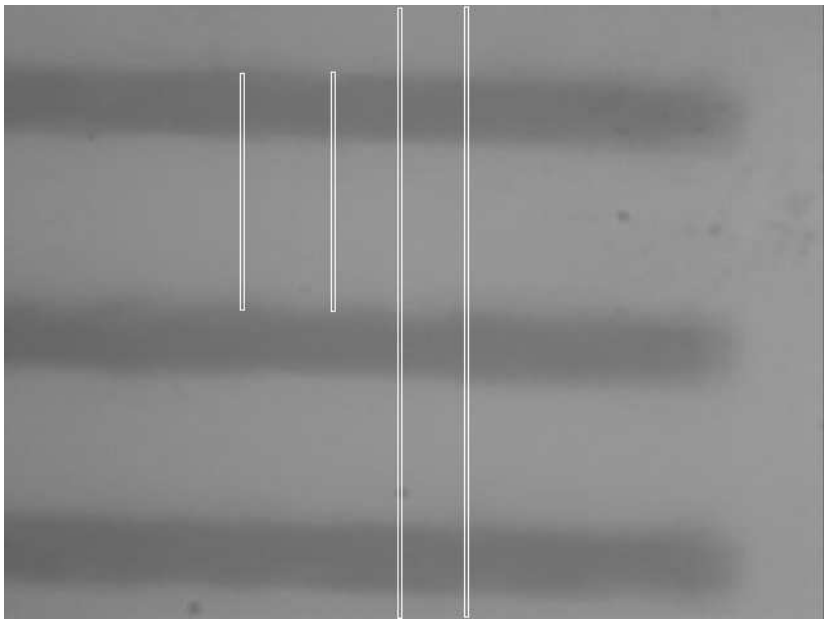

Figure 3-24: Ruler

The unit on the rule is 10 µm, and the pixels of the image were 2274 x 1704. The actual length of one unit on the image (shown in Figure 3-25, captured by the Canon camera under microscope) was 13 while the actual length of image in vertical was 668, so it was calculated that the magnification of the image was 0.30 µm/pixel.

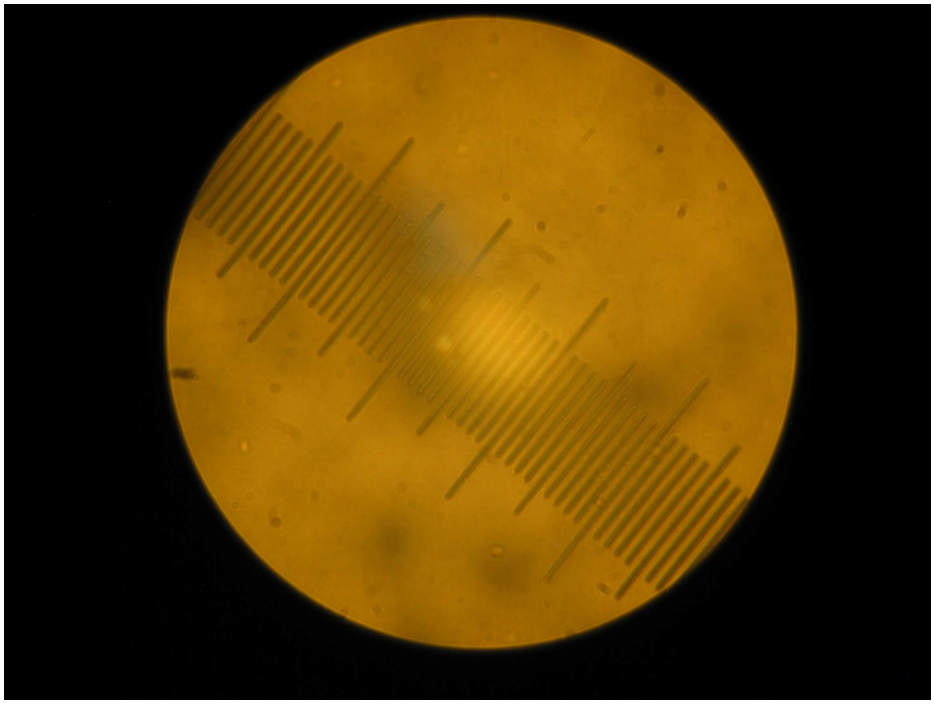

Figure 3-25: Scale on a microscope slide

3.8 Furnace Operation

The controller temperature was set at 900 ^{o}C for all the experiments in this thesis.

After the manufacturer's suggested bake out process was completed (see the details in Appendix I), the furnace was operated for experiments. It took about 2 hours to heat the furnace from laboratory room temperature to 900 ^{o}C. The heating rate could be adjusted by the 'OUTPUT PERCENT' switch on the temperature controller. The heating rates were 12 ^{o}C/min through the range of laboratory room temperature to 500 ^{o}C and 5 ^{o}C/min through the range of 500 ^{o}C to 900 ^{o}C. Figures 3-26 and 3-27 show the operating furnace in the laboratory.

The furnce cooled slowly after shut down. There was no additional cooling system to increase the cooling rate of the furnace. It took between 8-9 hours to drop the temperature from 900 ^{o}C to room temperature.

Figure 3-26: Operating furnace at controller temperature of 900 ^{o}C

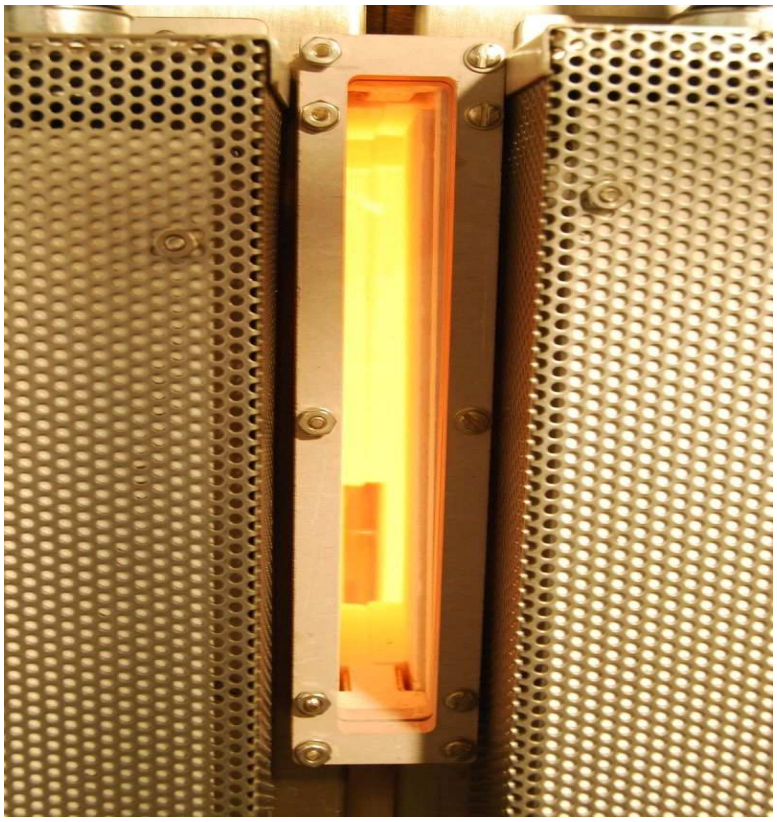

Figure 3-27: Heating zone during operation via view window

Chapter 4

Results

A study was performed to observe characteristics of fuel particles undergoing combustion in the furnace. Pulverized coal, wood, and switch grass were chosen to study a fossil fuel and two alternative fuels. In order to determine characteristics of different fuels, a standard microscope and a scanning electron microscope were used. The target size of particles used in the experiments was 90-106 μm.

Experiments were performed to determine the resolution and magnification in the field of view of the visualization system. Experiments were performed to evaluate the dropping rate of particles of the solid fuels. Temperatures in the retort during operation were also measured.

Pulverized coal, wood, and switch grass particles were stored in the injection needle, and dropped through the nozzle and into the furnace tube when vibration was applied. The camera system was located in front of the viewing window of the furnace to visualize the combustion of the fuel particles.

4.1 Furnace Operation Results

Temperature measurements were obtained using an OMEGA long-handle thermocouple to determine temperatures in the furnace retort tube. Figure 4-1 shows placement of the thermocouple tip at positions 4 and 10 cm below the water-cooled nozzle tip. Table 4-1 shows temperature measurement obtained at several temperature controller settings. For each of these measurements, the controller was set to the temperature shown and the furnace was allowed to remain at the set temperature for 20 minutes. The cooling water was supplied to the flanges and injection nozzle. Temperature T_1 was measured by placing the thermocouple 4 cm below the nozzle tip and T_2 was measured by 10 cm below the nozzle tip. It can be seen that on average, T_1 was 40 ^{o}C colder than controller temperature and T_2 was 20 ^{o}C colder. The delta values on the table is the difference between the controller temperatures and the measured temperatures. Temperature measured in the tube of the injection nozzle was on the average 30 ^{o}C. The bottom of the retort was capped during these measurements.

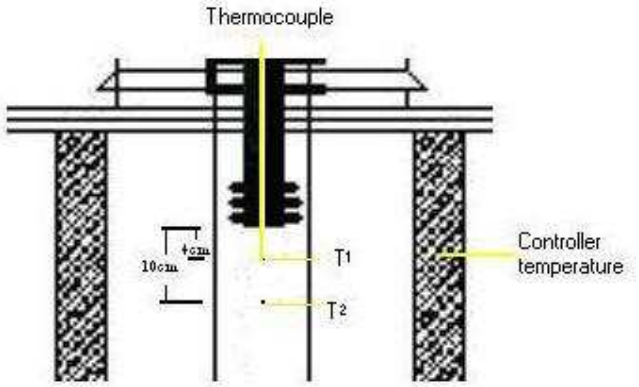

Figure 4-1: Schematic diagram of temperature measurement

Table 4-1: Controller temperature and temperatures in retort

Controller Temperature (^oC)	T_1 in retort (^oC)	Delta T_1 (^oC)	T_2 in retort (^oC)	Delta T_2 (^oC)
600	559	41	577	23
650	613	37	630	20
700	659	41	682	18
750	706	44	730	20
800	756	44	783	17
850	806	44	836	14
900	856	44	885	15

4.2 Particle Dropping Rate at Lab-Room Temperature Results

Experiments were performed to determine the particle dropping rates for the needle vibration delivery system at laboratory room temperature. The goal of these tests was to select needle sizes, vibration settings, and syringe placement for each fuel type such that individual particles would drop from the needle at rate of about one particle per second. No. 19, 20, 21, and 22 gauge needles were tested to drop particles of each fuel type. Large gauge needles were showed to let groups of particles fall through the needle, while small needle prevented particles dropping into the injection nozzle. Table 4-2 shows the optimum needle sizes and vibration settings for-each fuel type. Tables 4-3, 4-4 and 4-5 show test results for coal, wood, and switch grass particle dropping tests with the optimal gauge needles under different vibration setting and syringe placements. The vibrator speed range is 1 to 6. If the vibrator speed is too high, the needle tip would touch the inner wall of the injection nozzle tube during vibration. If the vibrator speed was too low, no particle would drop through the needle into the injection nozzle, but remain in the syringe. For each test, about 30 second of video was taken to record the fuel particle dropping using the Kodak camera and Nikon 60mm micro lens with the frame rate of 250 fps and the shutter speed of 1/10000 s.

Table 4-2: Optimum needle delivery system

	No. needle gauge	Inner diameter of needle	Vibrator setting	Needle angle	Needle height
Pulverized coal	21	0.495mm	5	90^o	50cm
Wood	20	0.584mm	5	90^o	37.5cm
Switch grass	20	0.584mm	5	60^o	50cm

Table 4-3: Coal particle dropping test with No 21 gauge needle

Vibration Range(4~6)	Needle Position(cm)	Needle Angle(90°,60°)	Clogging	Injection Rate	Particle Amount	Other Comment
3	50	90	No	Zero	Nothing	Nearly blocked in needle
4	50	90	No	Zero	Nothing	Nearly blocked in needle
5	50	90	No	Average	Small	Go everywhere
3	37.5	90	No	Average	Average	Nearly straight
4	37.5	90	No	Fast	Small	Go everywhere and separately
5	37.5	90	No	Zero	Nothing	N blocked in needle
3	25	90	No	Fast	Small	Hard to figure out the particles
4	25	90	No	Slow	Many	Group particles drop
5	25	90	No	Average	Small-group	Nearly straight
3	25	60	No	Zero	Nothing	No particle goes through
4	25	60	No	Zero	Nothing	No particle goes through
5	25	60	No	Slow	Average	Several groups drop
3	37.5	60	No	Slow	Small	Several groups drop
4	37.5	60	No	Average	Average	Nearly straight, drop one by one
5	37.5	60	No	Average	Many	Groups drop
3	25	60	No	Average	Several particles	Separately drop,
4	25	60	No	Average	Many	Go everywhere, groups drop
5	25	60	No	Fast	Many	Go everywhere, groups and pieces drop

Table 4-4: Wood particle dropping test with No 20 gauge needle

Vibration Range(4~6)	Needle Height(cm)	Needle Angle(90°,60°)	Clogging	Injection Rate	Particle Amount	Other Comment
4	25	90	Yes, little	Average	Average	Nearly straight, store at needle point
5	25	90	No	Fast	Many	Go everywhere
6	25	90	No	Fast	Only several pieces	Go everywhere
4	25	60	No	Slow	Small	Nearly straight
5	25	60	Yes, heavily	Average	From many to small	Nearly straight
6	25	60	Yes, little	Fast	Average	
4	37.5	90	No	Zero	Nothing	No particle goes through
5	37.5	90	No	Slow	Small	Store at needlepoint
6	37.5	90	Yes, little	Average	Small	Nearly straight
4	37.5	60	No	Zero	Nothing	No particle goes through
5	37.5	60	No	Average	Many	Go everywhere, store at needle point
6	37.5	60	No	Slow	Average	Store at needle point
4	50	60	No	Slow	Small	
5	50	60	No	Average	Average	Go everywhere
6	50	60	Yes, little	Fast	Many	Nearly same direction
4	50	90	No	Zero	Nothing	No particle goes through
5	50	90	No	Average	Many	Nearly same direction
6	50	90		Fast	Average	Go everywhere

Table 4-5: Switch grass particle dropping test with No 20 gauge needle

Vibration Range(4~6)	Needle Height(cm)	Needle Angle(90°,60°)	Clogging	Injection Rate	Particle Amount	Other Comment
4	25	90	No	Average	Small	Nearly straight
5	25	90	No	Average	Many	particles go everywhere
6	25	90	No	Fast	Many	Nearly straight
4	25	60	No	Average	Average	Particles go everywhere
5	25	60	No	Average	Average	Particles go everywhere
6	25	60	No	Fast	Many	A little store at needle point
4	37.5	60	Yes, little	Zero	Small	A little store at needle point
5	37.5	60	No	Fast	Many	Particles go everywhere
6	37.5	60	No	Fast	Many	A little store at needle point
4	37.5	90	No	Average	Small	Particles go everywhere
5	37.5	90	No	Average	From many to small	Particles go everywhere
6	37.5	90	No	Fast	Average	Nearly straight
4	50	60	Yes, little	Average	Nothing	Nearly stored at needlepoint
5	50	60	No	Average	Many	Go everywhere, store at needle point
6	50	60	No	Fast	Average	Particles go everywhere
4	50	90	No	Average	Nothing	Particles go everywhere
5	50	90	No	Fast	Average	Go everywhere
6	50	90	No	Fast	Small	Go everywhere

4.3 Particle Combustion at High-Temperature Results

Figures 4-2, 4-3, and 4-4 show images of fuel particles undergoing combustion in the furnace retort. These images are still frames taken from video obtained with the Cohu CCD camera with a frame rate of 30 fps and shutter speed of 1/4000 seconds. The Questar lens was used. The field of view of the camera was centered approximately 4 cm below the injection nozzle tip. The magnification of the images of combustion was 2.31 µm/pixel. The resolutions of the images were 31 µm/cycle in the vertical direction and 50 µm/cycle in the horizontal direction. The magnification value was used to provide the scale bar on each image. The controller temperature was set at 900 ^{o}C, and thus the temperature in the field of view is approximately 856 ^{o}C as was determined by thermocouple measurements (position T_1). The combustion gas was air at atmospheric pressure.

Figure 4-2 shows images of burning coal particles. Image (a) shows a burning particle falling in the furnace tube, and the size of the particle and its flame was approximately 60 µm. Image (b) shows one coal particle burning with a weak intensity, indicating that the particle is out of focus and not in the depth of field or that its flame is of low intensity. Images (c) and (d) show several particles burning with intense flames. The particles in images (e) and (f) show that the resolution of these images allows distinction between particle surface features and flames, and capability to measure the size and intensity of each feature.

Figure 4-3 shows images of burning switch grass particles. Images (a), (c), and (e) show multiple falling particles within the field of view, each particle can be

distinguished and the size and intensity of the flames can be determined. Images (b), (d) and (f) show single high-magnification burning switch grass particles, again, each showing the clarity and resolution that allows estimation of particle shape and flame intensity.

Figure 4-4 shows images of burning wood particles. Images (a) and (b) show very faint particles with the size of approximately 140 μm: these were either in the foreground or background (out of the depth of field) or they were particles that had not reached a temperature to begin burning of volatiles with high intensity flames. Images (c) and (d) shows wood particles with intense flames.

It was shown from the images that the burning particles had flames with different brightness (intensity) and different sizes, and the reasons could be that the burning particles were at different combustion stages, or some of them were in the focus of view and some of them were out of focus. Particles were infrequently in the field of view camera system, numerous particles combusted to the right and to the left of the field of view because they meandered as they fell due to thermal convection of the gas in the retort and due to forces resulting from the vibration of the nozzle tip. But in general it was typical to be able to obtain at least five clear images of particles during three or four minutes of video.

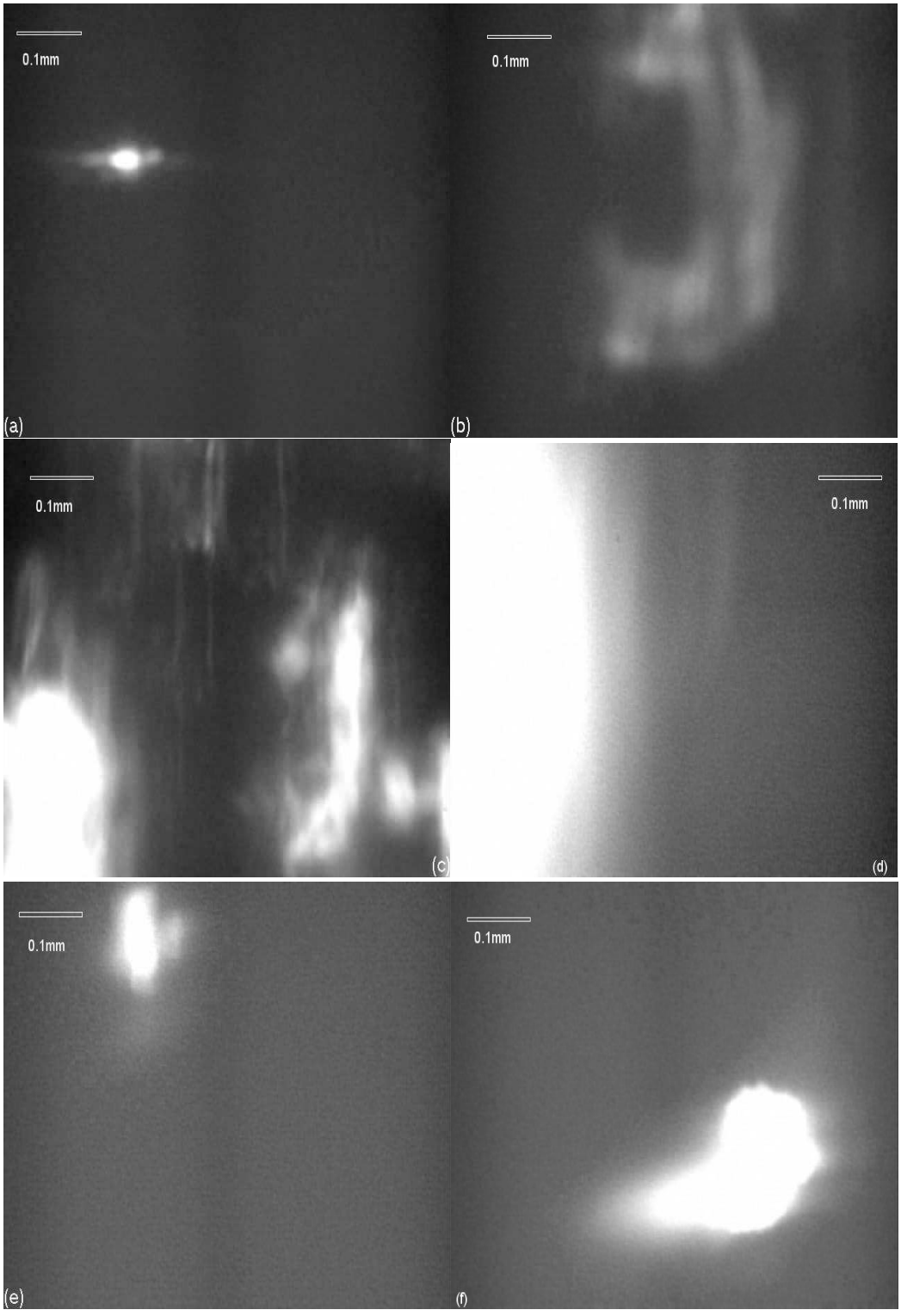

Figure 4-2: Burning coal particles at 856 ^{o}C

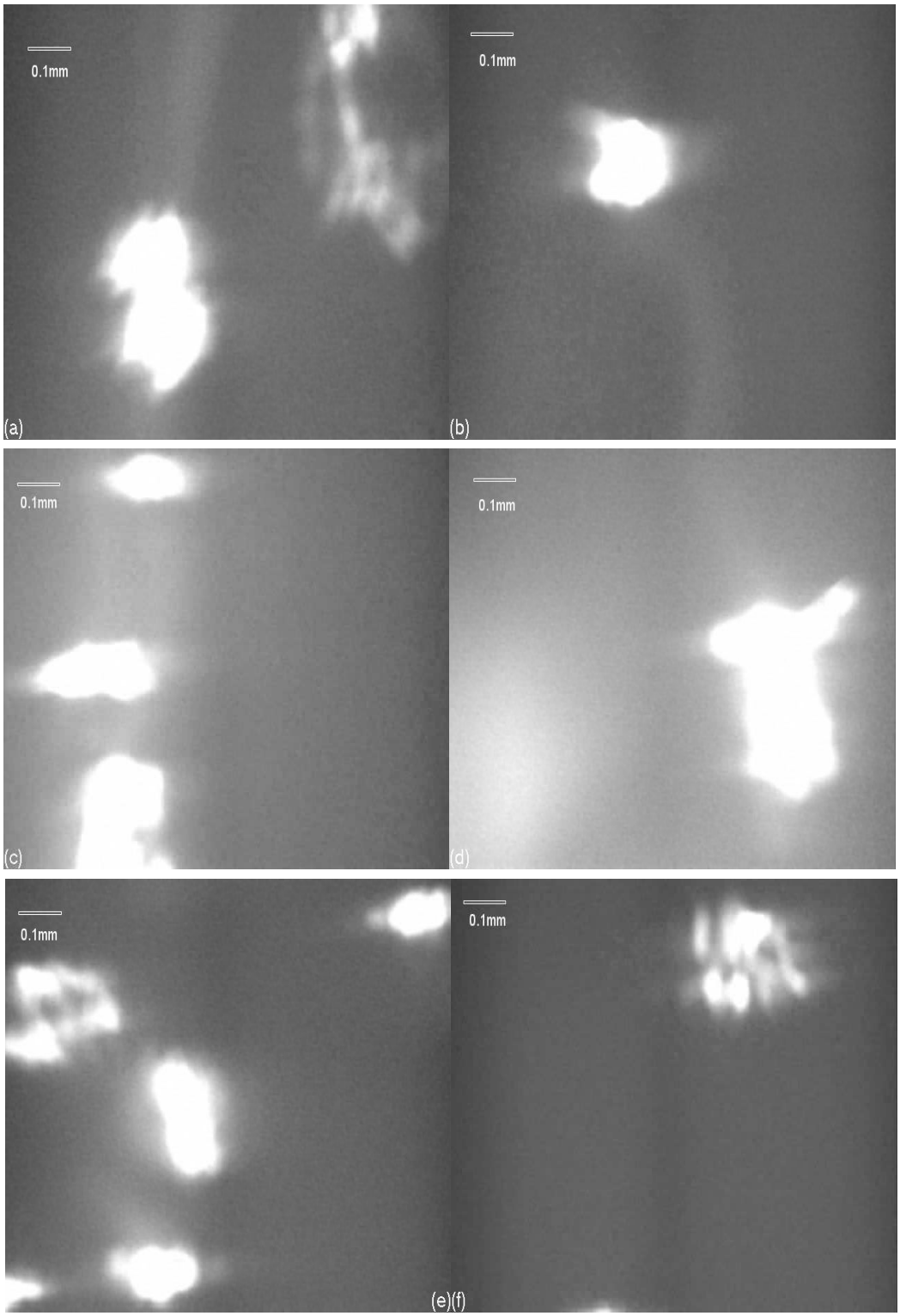

Figure 4-3: Burning switch grass particles at 856 ^{o}C

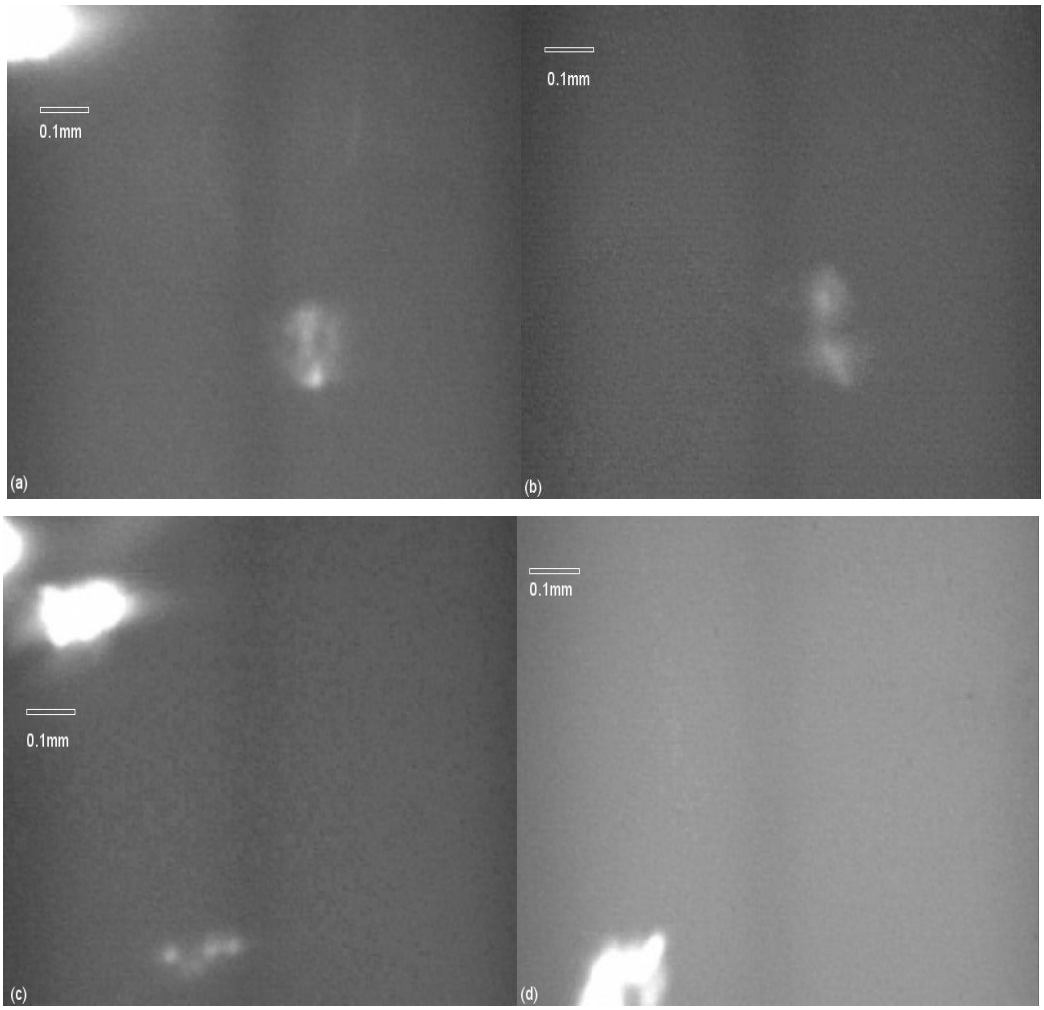

Figure 4-4: Burning wood particles at 856 ^{o}C

Chapter 5

Conclusions

A laboratory-scale burn simulator (a drop tube furnace) was designed and developed to study the combustion of solid fuel particles. Unique features of the system are three clear quartz windows on the sides of the furnace and a clear retort tube making it possible to obtain visualizations of falling particles undergoing combustion processes. A water system was designed and installed and it kept the flanges and nozzle cool, preventing the falling particles from burning in the nozzle, allowing all combustion to occur in the clear drop tube. An injection nozzle was designed and achieved delivery of individual fuel particles into the furnace. A number of camera systems and lenses were used, and the Questar lens was found to provide the needed image clarity and resolution for 100 μm particles undergoing combustion at 900 ^{o}C. A quartz glass retort from Ace Glass was determined to be needed to replace the original ATS quartz glass retort, because the ACE glass tube had a smoother finish, and resulted in less image distortion due to refraction.

We measured the temperature distribution in the retort during furnace operation with no imposed air flow, and the temperature in the center of the furnace retort was less than 40 ^{o}C lower than the temperatures readings on the furnace controller. We were able to achieve retort temperatures of approximately 900 ^{o}C (and

visualization at these temperatures) and thus achieved our goal of temperature in the retort that was similar to the temperature in the industrial cement production process where alternative fuels and coal are fed.

The syringe vibration system was successful at delivering fuel particles at a slow rate to the injection nozzle. Appropriate particle dropping rates required different vibration intensities and needle sizes for coal, wood and switch grass particles. Experiments determined that No. 21 gauge needles were selected for coal particle dropping while No. 20 needles were selected for wood and switch grass particles.

Clear and highly resolved images of coal, wood, and switch grass particles undergoing combustion at 900 ^{o}C in air were obtained. The magnification of these images was 2.31 µm/pixel and the resolution in the vertical direction was 0.031 mm/cycle and 0.050 mm/cycle in the horizontal direction. SEM and microscope images were obtained of the fuel particles before and after combustion.

Images of the burning particles revealed clarity and intensity contract sufficient to estimate particle size and shape, and flame properties. Particles meandered and moved from side-to-side as they fall through the tube because of the convective flows in the furnace; with the small field of view resulting from the high magnification this proved troublesome because particles were infrequently in the camera field of view. Nevertheless, the capability of the furnace and imaging system was demonstrated and found to be appropriate and validated the potential of the system to provide color images for surface temperature measurement.

Chapter 6

Recommendation for Future Work

Further studies may include additional modification to the visualization procedures and using new color camera systems to measure spatially and temporally temperature distributions on surfaces of fuel particles.

Observation and measurement of fuel particle temperatures and flame distributions in controlled combustion gas atmospheres will allow evaluation of combustion efficiency and effectiveness. Studies can be conducted to determine effects of fuel type, particle size, gas composition, gas temperature, and other process factors.

Bibliography

Akkapeddi, S., *Alternative Solid Fuels for the Production of Portland Cement*. Masters Thesis, Auburn University, Auburn, Alabama, 2008.

Alabama Forestry Commission, *Woody Biomass to Energy Opportunities in Alabama*. June 2009.

Atal, A. and Levendis, Y.A., Comparison of the Combustion Behavior of Pulverized Waste Tyres and Coal, *Fuel*. 74: 1570 (1995).

Baxter, L.L., Char Fragmentation and Fly Ash Formation during Pulverized-Coal Combustion, *Combustion and Flame*. 90: 174-184 (1992).

Beach, J., Elder, S. and Weeks, N., Case Study: Use of Circulating Fluidized Bed Boiler Byproduct to Solidify Oily Sludge, *2009 World Coal Ash Conference* (2009).

Bejarano, P.A. and Levendis, Y.A., Single-Coal-Particle Combustion in O_2/N_2 and O_2/CO_2 Environments, *Combustion and Flame*. 153: 270 (2008).

Boylan, D., Bush, V. and Bransby, D., Switchgrass Cofiring: Pilot Scale and Field Evaluation, *Biomass and Bioenergy*. 19: 411 (2000).

Clean Coal Technology Demonstration Program, Project Fact Sheets, U.S. Department of Energy, Office of Fossil Energy, (1996).

Courtemanche, B. and Levendis, Y.A., A Laboratory Study on the NO, NO*, SO*, CO

and CO_2 Emissions from the Combustion of Pulverized Coal, Municipal Waste Plastics and Tires. *Fuel*. 77: 183 (1998).

Davies, A.H.P., *Visualization of Flexographic and Offset Ink at Bubble Surfaces*, Masters Thesis, Auburn University, Auburn, Alabama, 2000.

Davies, A.H.P., Rossi, L., and Duke, S.R., A Method for Visualization and Measurement of Ink Adsorption Rates at Bubble Surfaces. Fundamentals and Numerical Modeling of Unit Operations in the Forest and Products Industry: *AIChE Symposium Series*. 324(96): 28 (2000).

Deutch, J. and Moniz, J., The Future of Coal: Options for a Carbon-Constrained World. *Massachusetts Institute of Technology Interdisciplinary Study* (2007).

Emerson, Z.I., Bonometti, T., Krishnagopalan, G.A., Duke, S.R., Visualization of Toner Ink Adsorption at Bubble Surfaces. *TAPPI Journal*. 5(4): 10-16 (2006).

EPA. *Inventory of U.S. Greenhouse Gas Emissions and Sinks: 1990-2002*. U.S. Environmental Protection Agency. Washington, DC. EPA 430-R-04-003 (2004).

Ernst Seed Catalog Web Page. *Switchgrass and Warm Season Grass Planting Guide. Ernst Conservation Seeds* (2007).

Fisher, J., Energy Density of Coal, *The Physics Factbook*, (2003).

Hanson, D., Mintzer, I., Laitner, J., Leonard, J.A., *Engines of Growth: Energy Challenges, Opportunities, and Uncertainties in 21st Century*. Argonne, III: Argone National Laboratory, (2004).

Hoadley, B., *Understanding Wood: a Craftsman's Guide to Wood Technology*, Taunton

Press, Newtown, CT, 2000.

Jackson, P.J., *Lea's Chemistry of Cement and Concrete*. 4th ed, London, 1998.

Jacott, M., Reed, C., Taylor, A., *Energy Use in the Cement Industry in North America: Emissions, Waste Generation and Pollution Control, 1990-2001*. Commission for Environmental Cooperation, 2nd North American Symposium on Assessing the Environmental Effects of Trade (2003).

Keefe, B.P., and Shenk, R.E., An Innovative Solution for Waste Utilization, *2003 IEEE Cement Industry Technical Conference.* Dallas, Texas: 197-226 (2003).

Kosmatka, S., Kerkhoff, B. and Panarese, W., *Design and Control of Concrete Mixtures*, Skokie, Illinois: Portland Cement Association, 2002.

Levendis, Y.A. and Estrada, K., Development of Multicolor Pyrometers to Monitor the Transient Response of Burning Carbonaceous Particles. *Rev. Sci. Instrum.* 63: 3608 (1992).

Levendis, Y.A. and Estrada, K.R., Development of Multicolor Pyrometer to Monitor the Transient Response of Burning Carbonaceous Particles, *Rev. Sci. Instrum*. 63(7): 3608 (1992).

Levendis, Y.A., Zhu, W., Wise, D.L., Simons, G.A., the Effectiveness of Calcium Magnesium Acetate (CMA) as a SOx Sorbent in Coal Combustion. *AIChE Journal*. 39: 761 (1993).

Livingston, S., *Visualization and Analysis of the Combustion of Alternative Fuels for the Replacement of Coal in Energy Production,* Undergraduate Honors Thesis, Auburn University, Auburn, Alabama, 2010.

Lu, H., Robert, W., Peirce, G., Ripa, Bryan, Baxter, L.L., Comprehensive Study of Biomass Particle Combustion, *Energy & Fuel,* 22(4): 2826-2839 (2008).

McLaughlin, B.S. and Kzos, L.A., Development of Switch grass (Panicum Virgatum) as a Bioenergy Feedstock in the United States, *Biomass and Bioenergy.* 28: 515 (2005).

Miura, T., *Advanced Coal Combustion*. Nova Science Publishers, Hauppauge, New York, 2001.

Oss, H. and Padovani, A., Cement Manufacturing and the Environment. *Journal of Industrial Ecology.* 6(1):89-106 (2002).

USGS, *Minerals Yearbook, Vol. 1. Metals and Minerals*, U.S. Geological Survey. U.S. Department of the Interior (2002).

Portland Cement Association. *Available at http://www.cement.org/index.asp* (2009).

Robinson, A. and Baxter, L., Pilot-scale Investigation of the Influence of Coal-biomass Co-firing on Ash Deposition. *Energy & Fuels*. 16: 343 (2002).

Ruth, L., Energy from Municipal Solid Waste: A Comparison with Coal Combustion Technology. *Prog. Energy Combust. Sci.* 24: 545 (1998).

Sami, M., Annamalai, K., and Wooldridge, M., Co-Firing of Coal and Biomass Fuel Blends, *Progress in Energy and Combustion Science*. 27: 171-214 (2001).

Samson, R., *Developing Energy Crops for Thermal Applications: Optimizing Fuel Quality, Energy Security and GHG Mitigation. In Biofuels, Solar and Wind as Renewable Energy Systems: Benefits and Risks.* Springer Science, Berlin, Germany. 395 (2008).

Samson, R. and Stamler, B.S., Going Green for Less: Cost-Effective Alternative Energy Sources. C.D. Howe Institute Commentary 282, *Economic Growth and Innovation*. 25 (2009).

Schilling, H.D., How Did the Efficiency of Coal Fired Power Station Evolve, and What Can Be Expected in the Future, *The Efficiency of Coal-Fire Power Station.* 1 (2005).

Stephens, A., *Visualization of Particle Formation Processes in Supercritical Fluids*, Master Thesis, Auburn University, Auburn, Alabama, 2003.

Taylor, H.F.W. *Cement Chemistry*, 2d, Thomas Thlford, London, 1997.

Teislev, B., Harboore-Woodchips Updraft Gasifier and 1500 KW Gas Engines Operation at 32% Effecincy in CHP Cofiguration, Babcock and Wilcox Volund R&D Center, 2002.

Tillman, D., Rossi, A. and Kitto, W., *Wood Combustion Principles, Processes, and Economics*, Academic Press, New York, 1981.

Tuin, S., *Visualization of Chlorella Algal Cells at Bubble Surface*, Master Thesis, Auburn University, Auburn, Al, 2008.

Wheatley, L., Levendis, Y.A, and Vouros, P., Exploratory Study on the Combustion and PAH Emissions of Selected Municipal Waste Plastics. *Environmental Science and Technology.* 27: 2885 (1993).

Yang, Y.B., Sharifi, V., Swithenbank, J., Combustion of a Single Particle of Biomass, *Energy & Fuels*. 22: 306 (2008).

Appendix A

Needle Gauge Comparison Chart

Needle	Nominal Outer Diameter			Nominal Inner Diameter		
Gauge	*mm*	*inches*	*tol. (in.)*	*mm*	*inches*	*tol. (in.)*
15	1.829	0.0720	±0.0005	1.372	0.0540	±0.0015
16	1.651	0.0650	"	1.194	0.0470	"
17	1.473	0.0580	"	1.067	0.0420	"
18	1.270	0.0500	"	0.838	0.0330	"
19	1.067	0.0420	"	0.686	0.0270	"
20	0.902	0.0355	+0.0005 -0.0000	0.584	0.0230	+0.0015 -0.0000
21	0.813	0.0320	"	0.495	0.0195	"
22	0.711	0.0280	"	0.394	0.0155	"
22s	0.711	0.0280	"	0.140	0.0055	"
23	0.635	0.0250	"	0.318	0.0125	"
24	0.559	0.0220	"	0.292	0.0115	"
25	0.508	0.0200	"	0.241	0.0095	"
25s	0.508	0.0200	"	0.140	0.0055	"
26	0.457	0.0180	"	0.241	0.0095	"
26s	0.467	0.0184	"	0.114	0.0045	"
27	0.406	0.0160	"	0.191	0.0075	"
28	0.356	0.0140	"	0.165	0.0065	"
29	0.330	0.0130	"	0.165	0.0065	"
30	0.305	0.0120	"	0.140	0.0055	"

(Source: Sigma-Aldrich Company)

Appendix B

Key Specifications of Furnace

Dimensions of furnace: 32.5cm W x 35cm H. x 75cm Long

Dimensions of retort: 6.25 cm I.D. x 97.5 cm Long

Heating Elements: Silicon carbide (SiC) "rammed rod"

Zones: Three zone 2600 watts per zone 55 amps/8000 watts total

Quartz View Port: 2.5 cm W x 22.5 cm Long. x 3

Flange Material: 304 Stainless Steel

Flanges: Integral type with water cooling, flange seals and flange

Appendix C

Kodak SR-500 Motion Corder Analyzer

Specifications

Input power: 110 or 220 volts

Shutter speed: 1/30 – 1/20000 sec

Max resolution: 512 x 480 pixels

Frame rate: 30 - 1000 fps

Gray scale: 256 levels

Lens mount: C-Mount

Sensor: 658 x 496 pixels

Frame storage: 546 full frames with standard memory

Appendix D

Nikon D40X DSRL Camera Specifications

Sensor Size: 15.6 x 23.7 mm^2

Image Sensor Type: CCD

Effective Pixels: 10.2 million

Shutter Speed: 30–1/4,000 sec

LCD Monitor Resolution: 230,000 dots

Weight: 495 g

Highest Expanded ISO Sensitivity: Hi1 (ISO 3200 equivalent)

Lens Mount: Nikon F mount with AF coupling and AF contacts

Picture Angle: Equivalent in 35 mm format is approx. 1.5X lens focal length

Dimension: 126 x 94 x 64 mm^3

LCD Monitor Type: TFT-LCD

Appendix E

COHU 2122 Monochrome Video Camera

Specifications

Pixels: 768 x 494

Pixel Size: 8.4 x 9.8 microns^2

Lens Mount: C/CS-mount

Operating Temperature: -10 to 500 ^oC

Weight: 200 g

S/N Ratio: >55dB

Shutter Speed: 1/60-1/10,000 s

Appendix F

File Batch

1) Download imaging from Kodak camera to computer.
2) Build a file with certain file name.
3) Save the group of imaging in the file.
4) Go to the folder the images are in, let the images shown in 5 rows. Click on the first file (f_000001.bmp) in the directory and then scroll down the 1st to the 606th file (f_000606.bmp) and click it holding the SHIFT key. Then do the operation to 3rd and 5th row according to select 60% of entire images. Make sure (save as new file) is highlighted.
5) Set the save folder to the folder you are taking images from, which makes the job easier in seeing the files already converted.
6) Click CTRL + A to select all the images, and then click right button to run rotate clockwise.
7) Once all the images are all rotated, close the file.

Appendix G

Movie Speed Setting

1) Once the batch change is done and all the images are converted, open Jasc Animation Shop to adjust the movie speed with the frame rate in the experiment.
2) Click on File > Animation Wizard.
3) Choose same size as the first image frame, click NEXT.
4) Choose transparent as the background canvas color, click NEXT.
5) Choose default setting, click NEXT.
6) Choose play 1 time and $1/100^{th}$ of a second to display each frame (fastest frame rate is 100 frame per second), click NEXT to complete the setting.

Appendix H

Movie Building Procedure

1) Once the movie setting is done, add images from the batch to the Animation Shop.
2) Click Add Image, find the batch saving the files, and then click on the first file (f_000500.bmp) in the directory and then scroll to the 500th file (f_000001.bmp).
3) Once the images are selected, click NEXT to complete the file selection.
4) Click View Animation on the top bar to preview the movie.
5) Once the quality of the movie and speed are good, click File > Save As.
6) Name the save file.
7) Save as: AVI.
8) The movie building takes about 3-5 minutes to complete depending on memory load and number of frames.
9) Make sure save the movie in the right batch.
10) When the building is done it shows the movie in the saved batch. To open the movie, go to the directory and double click it. Windows Media Player opens it up and plays the 100 frames per second movie.

Appendix I

Furnace Bake Out Procedure

1) Mount retort into furnace. Vent retort during bake.

2) The first time the furnace is fired, heat up to 900 ^{o}C. The heating up rate can be rapid from room temperature to 500 ^{o}C (about 5 ^{o}C/min), and 3 ^{o}C/min from 500 ^{o}C to 900 ^{o}C. Let the furnace sit at the temperature for about two hours.

3) Increase the furnace temperature to 1200 ^{o}C at a rate of 80 ^{o}C/hr. Let furnace sit for about one hour at this temperature.

4) After temperature is reached, let the furnace sit. To shut down the furnace, shut off power and with door or end caps closed, allow the furnace to slowly cool 8–10 hours or overnight before opening.

Appendix J

Resolution and Magnification Results

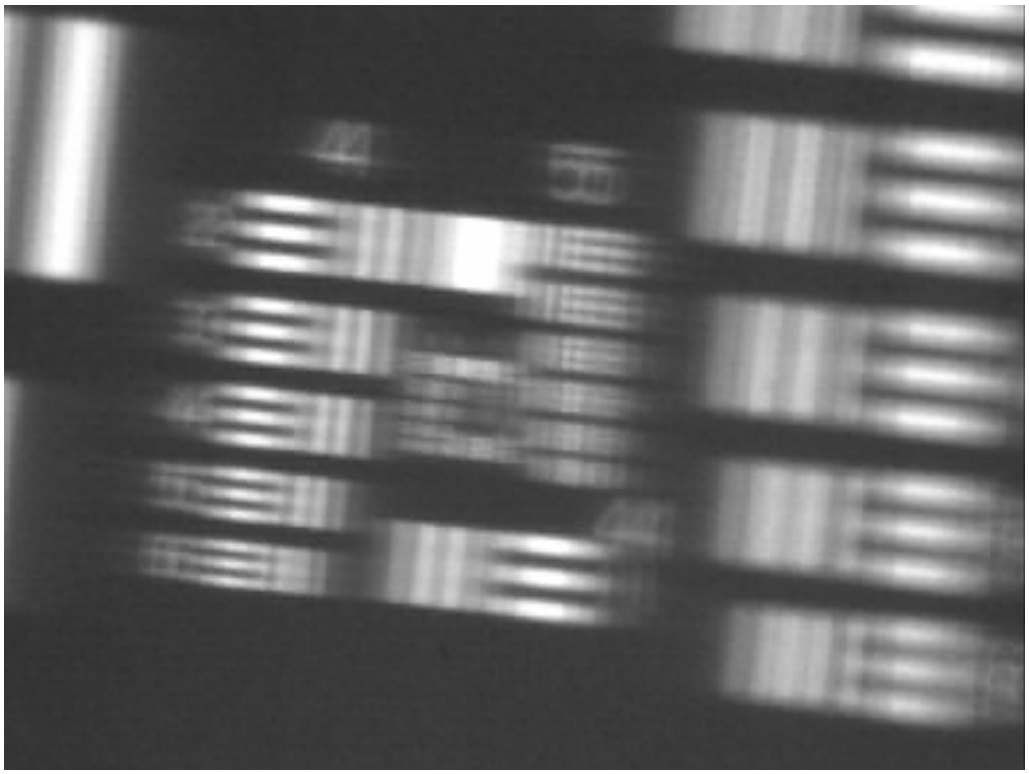

Figure J-1: USAF 1951 resolution test pattern (from Edmund)

The USAF 1951 resolution test pattern was vertically inserted into the retort in the furnace. The target was located in the field of view of the camera; the camera was set up in front of the view window with the distance of 13 inches to the target. Images were obtained at laboratory room temperature. Cohu camera and Questar lens were used. The smallest resolved bars in the vertical direction was Group Five, Element

One, with the resolution values - $\frac{32cycle}{mm}$, so the resolution of the image in vertical was calculated: $\frac{mm}{32cycle}$ = 31µm. In horizontal, the smallest resolved bars was Group Four, Element Three with a resolution value $\frac{20.16cycle}{mm}$, so the resolution of the image: $\frac{mm}{20.16cycle}$ = 50 µm.

Table J-1: USAF 1951 resolution test chart (from Edmund)

Number of Line Pairs / mm in USAF Resolving Power Test Target 1951												
Group Number												
Element	-2	-1	0	1	2	3	4	5	6	7	8	9
1	0.250	0.500	1.00	2.00	4.00	8.00	16.00	32.0	64.0	128.0	256.0	512.0
2	0.280	0.561	1.12	2.24	4.49	8.98	17.95	36.0	71.8	144.0	287.0	575.0
3	0.315	0.630	1.26	2.52	5.04	10.10	20.16	40.3	80.6	161.0	323.0	645.0
4	0.353	0.707	1.41	2.83	5.66	11.30	22.62	45.3	90.5	181.0	362.0	-----
5	0.397	0.793	1.59	3.17	6.35	12.70	25.39	50.8	102.0	203.0	406.0	-----
6	0.445	0.891	1.78	3.56	7.13	14.30	28.50	57.0	114.0	228.0	456.0	-----

Appendix K

Coal Sample Results from ROBERTA Plant

Table K-1: Cement plant results for coal samples

Test	Parameter	Value (wt. %)
Proximate Analysis	Ash	18.78
	Fixed Carbon	53.85
	Volatile Matter	27.37
Ultimate Analysis	Carbon	70.28
	Hydrogen	4.29
	Nitrogen	1.38
	Oxygen	3.61
	Sulfur	2.6
Standard Parameters	Al_2O_3	24.03
	CaO	6.30
	Fe_2O_3	9.86
	K_2O	2.33
	MgO	1.10
	Na_2O	0.17
	SiO_2	48.1
	SO_3	6.51
Heat Value [1]		12169

Notes: [1] Value is reported as BTU/lb.

Appendix L

Particle Dropping at Lab-room Temperature

The high-speed video allowed estimation of the particle dropping velocity.

With the given conditions: average particle size of 100 µm, high speed camera frame rate of 250 fps, shutter speed of 1/10000 s, No. 20 gauge needle nominal outside diameter of 900 µm.

Then software-ImageJ was used to estimate the dropping particle rate at different vibration speeds and Window Paint was used to draw the captured images. Here, three heights were chosen to hold the needle. The first height was 25cm higher than the vibrator at the bottom of the metal stand that fixed the injection needle; the second height was 37.5 cm higher than the vibrator while the third height was 50cm higher as shown in Figure 3-16. Different heights on the clamp obtained different vibrating intensity. The vibrator had a vibration speed range from 1 to 6, 1 being the lowest and 6 being the highest vibration intensity. One sample was analyzed to estimate the particle dropping rate (wood particles, No. 20 gauge needle): height at 25 cm, vibration speed of 4. In Figure L-1, A, B and C were different spots (different distances to the bottom of the needle) of particles after dropping via the nozzle. The

scale on the particle showed the real size of each particle on the image.

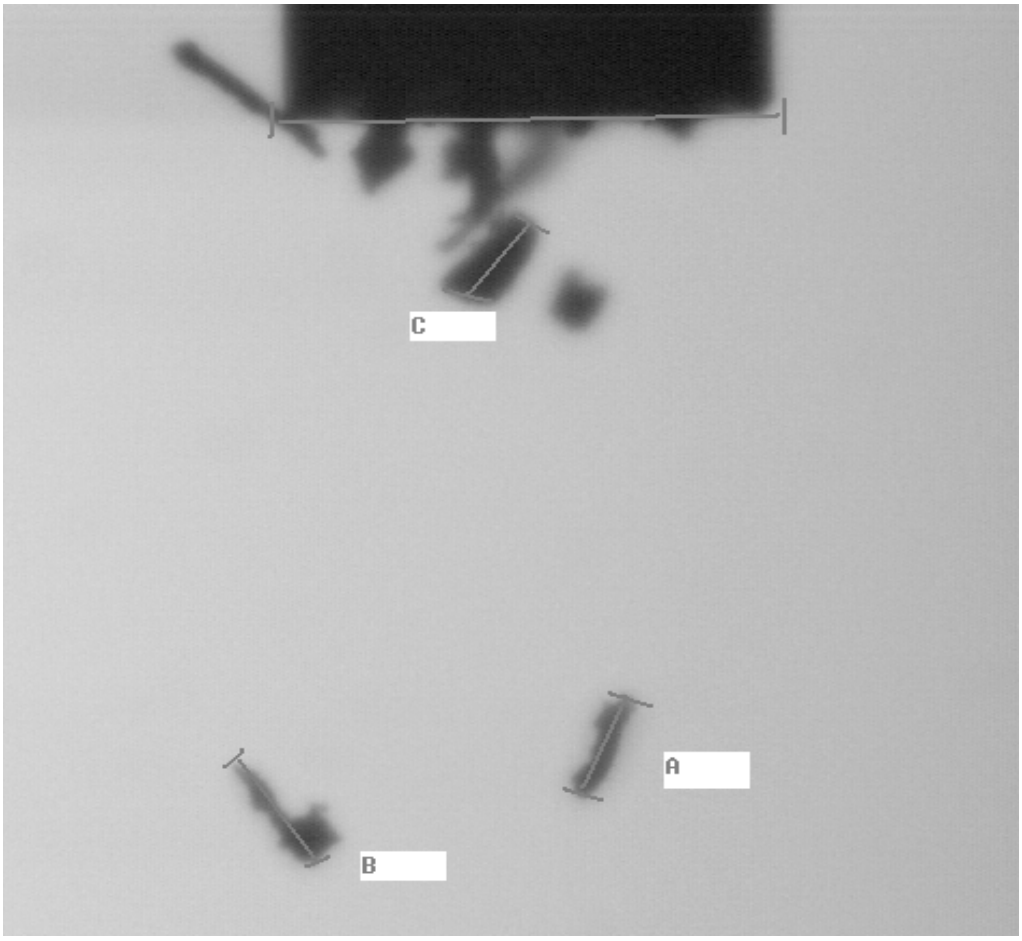

Figure L-1: Dropping particles at laboratory-room temperature

Figure L-1 shows sample image to calculate the resolution of wood particles. These images were captured in the retort by the KODAK camera with NIKON 60mm micro lens. The details about resolution of particles were shown in Appendix J. Hence, the resolution of KODAK camera with NIKON 60mm micro lens was 62.5 µm/cycle.

On Figure L-2, the needle was set at an angle of 35º, vibration speed at 5 and the needle height of 50 cm. The camera was set with the frames rate of 250 fps, and the video was built up at 100 fps.

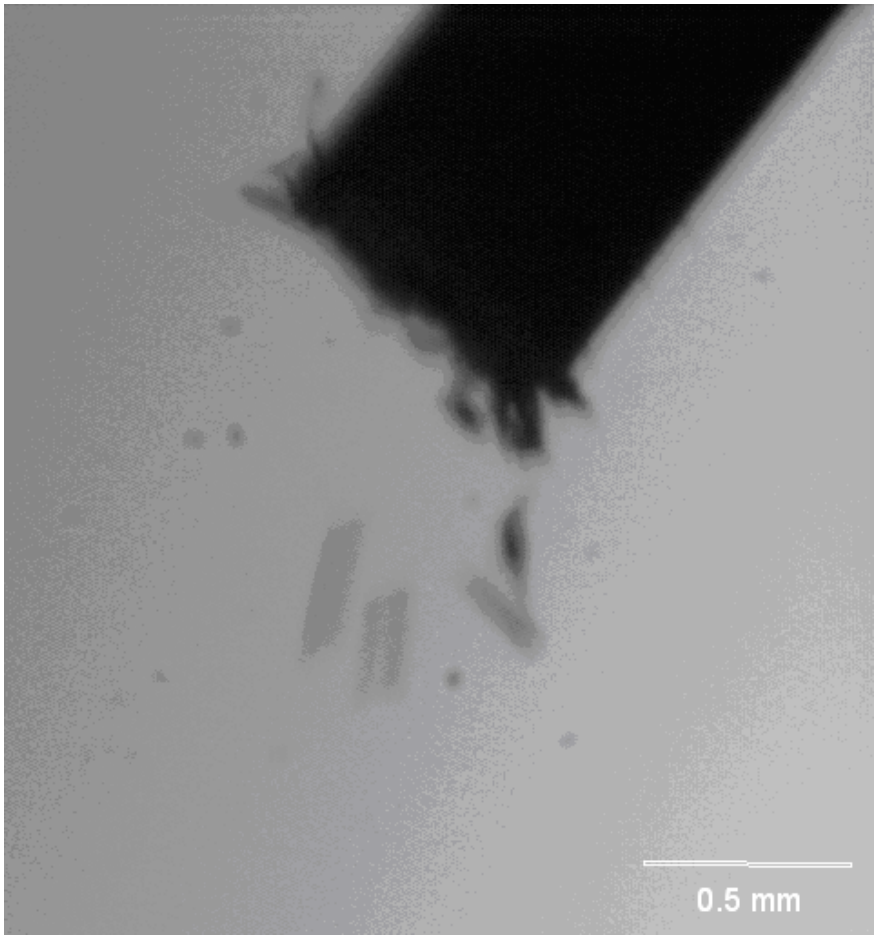

Figure L-2: Dropping coal particles with needle at the angle of 35º

In Figure L-3, the needle was set vertically, the vibration speed at 5 at the height of 37.5 cm. The camera was set with the frame rate of 250 fps. After observing and comparing the two set ups, more particles were dropping based on qualitative observation in same time at the height of 37.5 cm.

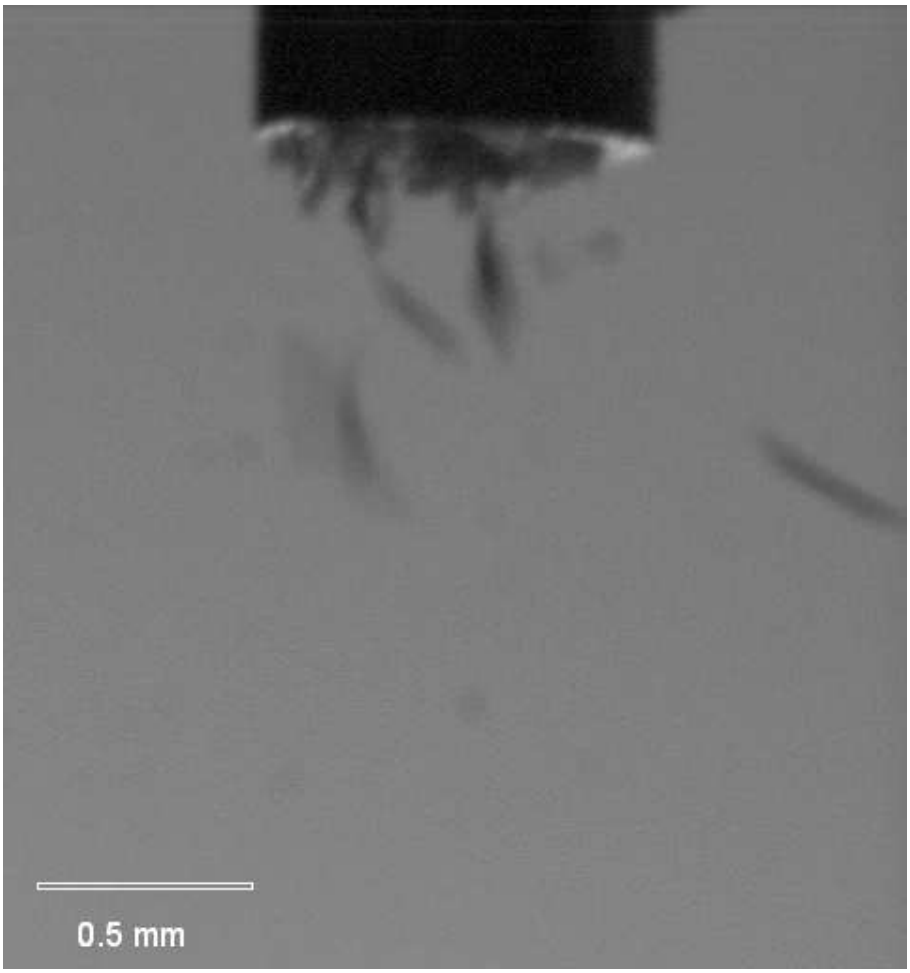

Figure L-3: Dropping wood particles with vertical needle